

INVITED PAPER

PACS numbers: 42.55.Lt; 42.60.Da; 42.65.Sf
DOI: 10.1070/QE2008v038n01ABEH013205

Phase instability in a four-frequency anisotropic-ring cavity gas laser

L.P. Svirina

Abstract. **The nonlinear dynamics of a class A four-frequency ring gas laser with elliptic nonorthogonal states of counterpropagating waves is studied based on a developed and experimentally tested model taking explicitly into account the dependence of the backscattering coefficient of counterpropagating waves on polarisation characteristics. It is shown that the instability of phase characteristics of the generated field cause the switching of the intensities, polarisation states, and phase differences of counterpropagating waves in the self-oscillation regime, the shift of the intensity switching over detuning caused by the phase shift of the wave due to nonzero ellipticity, the spontaneous phase symmetry breaking accompanied by the appearance of deterministic and noise-induced chaos, the multistability of attractors with different topologies, and symmetric and asymmetric chaotic, as well as stochastic oscillations.**

Keywords: *polarisation of light, linear coupling, ring laser, multimode lasing, spontaneous break of the phase symmetry, symmetric and asymmetric chaos, noise-induced complicated oscillations.*

1. Introduction

The application of class A four-frequency ring gas lasers (FRGLs) in gyroscopes (see, for example, [1 – 3]) attracts persistent interest in the study of the role of various physical mechanisms in the formation of a generated field and in the development of new methods for controlling radiation parameters of these lasers. The FRGL model based on the matrix method and used in this paper allows one to study the influence of polarisation effects on the operation parameters of laser gyros. Aside from conventional technical applications, an anisotropic-cavity FRGL is an excellent physical model for studying general properties inherent in multiparameter high-dimensional nonlinear systems.

So far the studies of FRGLs were mainly restricted to the stationary lasing regimes (see, for example, [4 – 6]), while backscattering was taken into account only for counterpropagating waves with coincident linear polarisation states [5]. The features of the nonlinear dynamics in such systems were experimentally found comparatively recently [7, 8]. In this paper, the equation are derived which describe the operation of FRGLs taking into account backscattering for arbitrary polarisation states of counterpropagating waves and conditions for the development of regular, chaotic, and stochastic lasing regimes are determined in the case of the elliptic nonorthogonal polarisation states of these waves.

In anisotropic-cavity lasers with the adiabatic exclusion of populations and polarisability of the medium (class A lasers), the two physical mechanisms are known which give rise, in the absence of any external time-dependent action, to self-oscillation lasing regimes: these are a linear coupling of counterpropagating waves, producing the phase instability, and the competition between the anisotropy of the nonlinear active medium and the cavity anisotropy, resulting in the polarisation instability.

The linear coupling of generated waves appearing due to their backscattering by inhomogeneities of the medium and cavity involves the phase characteristic of radiation to the laser field formation and creates prerequisites for the appearance of effects caused by the phase instability, which can be also observed in lasers with a scalar field (see, for example, [9 – 12]). The undamped periodic oscillations of polarisation characteristics of light appear when the cavity and medium anisotropies are comparable and the polarisation eigenstates of the medium and cavity strongly differ from each other (in this case, the equations for intensities, azimuths, and ellipticities are independent of the laser wave phases [13]). The polarisation instability was observed experimentally at different transitions in linear He – Ne [14 – 17] and He – Xe lasers, and was described theoretically in [17, 18].

At present, despite the appearance of a number of papers in which the linear coupling in class B anisotropic lasers is taken into account (see, for example, [19, 20]), the properties of the vector field in laser systems caused by the instability of the phase characteristics of generated waves have not been adequately investigated.

Among important and virtually undeveloped problems of the modern dynamics of laser systems is the development of theoretical methods to describe anisotropic lasers with a linear coupling in the case of multimode oscillation. Also, the mechanisms of the appearance of complicated (chaotic and stochastic) lasing regimes in nonlinear systems with symmetry, which are promising for applications in optical data processing and communication systems, have not been sufficiently explored. The study of the nonlinear dynamics in FRGLs with linearly coupled elliptically polarised counter-

L.P. Svirina B.I. Stepanov Institute of Physics, National Academy of Sciences of Belarus, prosp. Nezavisimosti 68, 220072 Minsk, Belarus; e-mail: lsvirina@dragon.bas-net.by

Received 30 January 2006; revision received 6 June 2006
Kvantovaya Elektronika **38** (1) 1 – 15 (2008)
Translated by M.N. Sapozhnikov

propagating waves performed in this paper can be useful for solving all the above-mentioned problems of laser physics and can form the basis for understanding the properties of the nonlinear dynamics of various high-dimensional coupled physical systems.

2. The mathematical model

The linear coupling of counterpropagating waves in ring lasers caused by backscattering from inhomogeneities in the active medium and laser cavity, due to which the electromagnetic field in each of the propagation directions represents a superposition of these waves, is one the of the basic mechanisms of formation of the electromagnetic field in lasers with various active media. Backscattering of light in laser gyros at small rotation velocities leads to the equality of the frequencies of counterpropagating waves and the absence of a beat signal, i.e. the synchronisation effect or frequency locking (see, for example, [21, 22]).

Due to a variety of factors leading to backscattering (see, for example, [23–27]), the contribution of each of them to the laser field formation cannot be taken into account. At present this effect is described by two methods. The first one is based on the assumption [28, 29] that all the ordered inhomogeneities can be represented by a single anisotropic reflector in the general case located inside the cavity with the effective coupling coefficients between counterpropagating waves. In this case, it is necessary to take into account the boundary conditions on the reflector. The second method describes the influence of backscattering with the help of an external anisotropic mirror (see, for example, [30]).

The use of the Jones vector and matrix formalism [31–33] in the theory of gas lasers [34–38] allows one to take into account, within the framework of the first method, backscattering of waves with arbitrary polarisation states. Note that the matrix method was also used to solve one of the fundamental problems of the physics of anisotropic laser systems, namely, to take into account the equal influence of the anisotropy of the medium and the anisotropy of the laser cavity on the formation of polarisation of generated radiation and to describe experimental regimes with the azimuth and ellipticity periodically varying in time [17].

Figure 1 shows the scheme of an anisotropic-cavity FRGL and the configuration of the electromagnetic field on a reflector. The cavity contains reflector (*1*) – an optical inhomogeneity described by the complex reflection ($r^{\pm}$) and transmission ($t^{\pm}$) coefficients, which are different for counterpropagating waves in the general case and can depend, due to the possible presence of the diffusion component of scattered radiation and diffraction effects, on the polarisation states of generated waves.

The electromagnetic field in a single-mode FRGL* is described by the superposition of four travelling waves with the Jones vectors having the form [39, 34]

$$\boldsymbol{E}_j^i = \left[\frac{I_j^i(t)}{\cosh 2\beta_j^i(t)}\right]^{1/2} \begin{pmatrix} \cos z_j^i(t) \\ \sin z_j^i(t) \end{pmatrix} \times$$

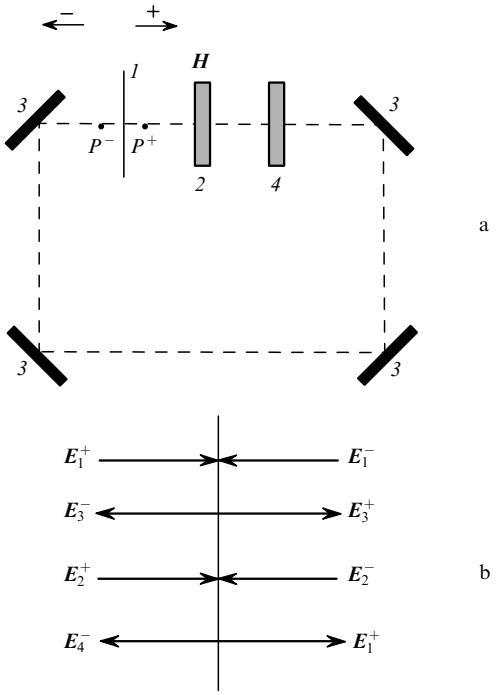

Figure 1. Scheme of an anisotropic-cavity ring gas laser with linear coupling (a) and the electromagnetic field configuration on a reflector element (b): (*1*) reflector element; (*2*) active medium; (*3*) mirrors; (*4*) anisotropic elements; $\boldsymbol{H}$ is the longitudinal magnetic field strength in the medium.

$$\times \exp[\mathrm{i}(\Psi_j^i(t) - \omega_j^i t)], \quad j = 1, 2, \; i = \pm, \tag{1}$$

where $I = |E|^2$ is the intensity; Ψ is the phase; $\omega/2\pi$ is the lasing frequency (in hertz); $z = \gamma + \mathrm{i}\beta$; γ is the azimuth; $\xi = \tanh\beta$ is the ellipticity of an electromagnetic wave; indices 1 and 2 correspond to unidirectional waves, and $\pm$ – to counterpropagating waves.

Let us write in the vector form the equations for stationary regime of lasing in the FRGL, which represent the conditions of reproducibility of the field vector after a round trip of light in the cavity (from the initial to final point). By starting from the point $P^{\pm}$ in the direction $\pm$, under the condition of the continuity of the tangential component of the electric field strength vector on the boundary of the effective reflector, we obtain

$$\hat{M}^+\hat{S}_1^+\boldsymbol{E}_3^+ = \lambda_1^+\boldsymbol{E}_1^+, \quad \boldsymbol{E}_3^+ = t_1^+\boldsymbol{E}_1^+ + r_1^-\boldsymbol{E}_1^- + \alpha(t_2^+\boldsymbol{E}_2^+ + r_2^-\boldsymbol{E}_2^-), \tag{2}$$

$$\hat{M}^+\hat{S}_2^+\boldsymbol{E}_4^+ = \lambda_2^+\boldsymbol{E}_2^+, \quad \boldsymbol{E}_4^+ = \alpha(t_1^+\boldsymbol{E}_1^+ + r_1^-\boldsymbol{E}_1^-) + t_2^+\boldsymbol{E}_2^+ + r_2^-\boldsymbol{E}_2^-, \tag{3}$$

$$\hat{S}_1^-\hat{M}^-\boldsymbol{E}_3^- = \lambda_1^+\boldsymbol{E}_1^-, \quad \boldsymbol{E}_3^- = t_1^-\boldsymbol{E}_1^- + r_1^+\boldsymbol{E}_1^+ + \alpha(t_2^-\boldsymbol{E}_2^- + r_2^+\boldsymbol{E}_2^+), \tag{4}$$

$$\hat{S}_2^-\hat{M}^-\boldsymbol{E}_4^- = \lambda_2^-\boldsymbol{E}_2^-, \quad \boldsymbol{E}_4^- = t_2^-\boldsymbol{E}_2^- + r_2^+\boldsymbol{E}_2^+ + \alpha(t_1^-\boldsymbol{E}_1^- + r_1^+\boldsymbol{E}_1^+), \tag{5}$$

*In the FRGL under study, an electromagnetic field is formed with one longitudinal and one transverse mode indices. The appearance of phase anisotropy in the cavity removes the degeneracy of this mode, thereby producing conditions for the existence above the threshold of four travelling waves with different intensities, frequencies, and polarisation states.

where $\hat{S}_1^{\pm}$ and $\hat{S}_2^{\pm}$ are the Jones matrices of the active medium for waves $1^{\pm}$ and $2^{\pm}$, respectively; λ_j^i are the eigenvalues of Jones matrices $\hat{Q}_{1,2}^{+} = \hat{M}^{+}\hat{S}_{1,2}^{+}$ and $\hat{Q}_{1,2}^{-} = \hat{S}_{1,2}^{-}\hat{M}^{-}$; $\hat{M}^{\pm}$ are the cavity matrices for directions $\pm$; $r_1^{\pm}$, $t_1^{\pm}$ ($r_2^{\pm}$, $t_2^{\pm}$) are the complex reflection and transmission coefficients, respectively, for counterpropagating waves belonging to the same eigenfrequency ω_{1c} (ω_{2c}) of the cavity; and α is a parameter describing the linear coupling of counterpropagating waves belonging to different eigenfrequencies of the cavity.

The absolute values of parameters $r_{1,2}^{\pm}$, $t_{1,2}^{\pm}$ satisfy the condition $|r_{1,2}^{\pm}|^2 + |t_{1,2}^{\pm}|^2 \leqslant 1$, and the phases $\phi_{1,2}^{\pm} = \arg r_{1,2}^{\pm}$ of the equivalent reflection coefficients upon scattering by the inhomogeneities of the permittivity and conductivity are related by the expressions $(\phi_{1,2}^{+} + \phi_{1,2}^{-})/2 = m\pi$ (m is an integer) in the case of the conservative coupling or by $(\phi_{1,2}^{+} + \phi_{1,2}^{-})/2 = (1/2 + m)\pi$ in the case of the nonconservative (dissipative) coupling, which is realised, as a rule, in experiments. In particular cases for $r = 1$, $t = 0$ and $r = 0$, $t = 1$ lasing equations (5) describe an ideal linear and an ideal ring lasers, respectively. In intermediate cases, the system has the properties both of linear and ring lasers.

The equations of nonstationary operation of a FRGL in the vector representation can be written in the form [40]

$$\frac{\mathrm{d}}{\mathrm{d}t'}\begin{pmatrix} \boldsymbol{E}_1^{+} \\ \boldsymbol{E}_1^{-} \\ \boldsymbol{E}_2^{+} \\ \boldsymbol{E}_2^{-} \end{pmatrix} = \begin{pmatrix} \hat{M}^{+}\hat{S}_1^{+}t_1^{+} & \hat{M}^{+}\hat{S}_1^{+}r_1^{-} & \hat{M}^{+}\hat{S}_1^{+}\alpha t_2^{+} & \hat{M}^{+}\hat{S}_1^{+}\alpha r_2^{-} \\ \hat{S}_1^{-}\hat{M}^{-}r_1 + & \hat{S}_1^{-}\hat{M}^{-}t_1^{-} & \hat{S}_1^{-}\hat{M}^{-}\alpha r_2^{+} & \hat{S}_1^{-}\hat{M}^{-}\alpha t_2^{+} \\ \hat{M}^{+}\hat{S}_2^{+}\alpha t_1^{+} & \hat{M}^{+}\hat{S}_2^{+}\alpha r_1^{-} & \hat{M}^{+}\hat{S}_2^{+}t_2^{+} & \hat{M}^{+}\hat{S}_2^{+}r_2^{-} \\ \hat{S}_2^{-}\hat{M}^{-}\alpha r_1^{+} & \hat{S}_2^{-}\hat{M}^{-}\alpha t_1^{-} & \hat{S}_2^{-}\hat{M}^{-}r_2^{+} & \hat{S}_2^{-}\hat{M}^{-}t_2^{-} \end{pmatrix} \times \begin{pmatrix} \boldsymbol{E}_1^{+} \\ \boldsymbol{E}_1^{-} \\ \boldsymbol{E}_2^{+} \\ \boldsymbol{E}_2^{-} \end{pmatrix} - \begin{pmatrix} \boldsymbol{E}_1^{+} \\ \boldsymbol{E}_1^{-} \\ \boldsymbol{E}_2^{+} \\ \boldsymbol{E}_2^{-} \end{pmatrix}, \tag{6}$$

where $t' - tc/L$ is the number of round trips of light in the cavity for the time t; c is the speed of light; and L is the cavity length.

The Jones matrix of a nonlinear homogeneous* active medium of the laser is defined as

$$\hat{S}_j = \exp\left(-\mathrm{i}\frac{\omega l}{c}\sqrt{\hat{\varepsilon}_j}\right) = \exp\left[-\mathrm{i}\frac{\omega l}{c}(1 + 2\pi\chi)_j\right], \tag{7}$$

where l is the medium length; ω/c is the wave number; $\hat{\varepsilon}$ and $\hat{\chi}$ are the two-dimensional projections of the permittivity and susceptibility tensors on the light propagation direction.

The Jones matrix of the active medium of a FRGL for the wave 1^{+} in the presence of a longitudinal magnetic field has the form [34, 38]

$$\hat{S}_1^{+} = \exp\left[-\mathrm{i}\frac{\omega l}{\hat{c}}(1 + 2\pi\hat{\chi}_1^{+})\right] = \exp h_1^{+} \exp \hat{H}_1^{+}, \tag{8}$$

where

$$-2\pi\mathrm{i}\hat{\chi}_1^{+}\frac{\omega l}{c} = k_0 l\left\{\bar{W}_1^{+}\hat{I} + \begin{pmatrix} 0 & -\mathrm{i}\Delta W_1^{+} \\ \mathrm{i}\Delta W_1^{+} & 0 \end{pmatrix} - \hat{I}c_1^{+\prime}I_1^{\prime +} - \mathrm{i}c_1^{+\prime\prime}I_1^{\prime +}\begin{pmatrix} 0 & -1 \\ 1 & 0 \end{pmatrix} - \sum_{\substack{j=1,i=-\\ j=2,i=\pm}} a_{1j}^{+i}I_j^{\prime i} - a_{1k}^{+}I_{1k}^{\prime +} - \sum_{\substack{j=1,i=-\\ j=2,i=\pm}} \begin{pmatrix} b_{1j}^{+i}/\cosh 2\beta_j^i & \tilde{b}_{1j}^{+i}/\cosh 2\beta_j^i - \mathrm{i}d_{1j}^{+i} \\ \tilde{b}_{1j}^{+i}/\cosh 2\beta_j^i + \mathrm{i}d_{1j}^{+i} & -b_{1j}^{+i}/\cosh 2\beta_j^i \end{pmatrix} I_j^{\prime i} - \begin{pmatrix} b_{1k}^{+}/\cosh 2\beta_k & \tilde{b}_{1k}^{+}/\cosh 2\beta_k - \mathrm{i}d_{1k}^{+} \\ \tilde{b}_{1k}^{+}/\cosh 2\beta_k + \mathrm{i}d_{1k}^{+} & -b_{1k}^{+}/\cosh 2\beta_k \end{pmatrix} I_{1k}^{\prime +}\right\}; \tag{9}$$

$I_{1,2}^{\prime\pm} = I_{1,2}^{\pm}|d_{ab}|^2/3\hbar^2\gamma_a\gamma_b$ are the dimensionless intensities of the waves $1^{\pm}, 2^{\pm}$; $I_{1,2}^{\pm} = |\boldsymbol{E}_{1,2}^{\pm}|^2$; $k_0 = 2\pi^{3/2}N|d_{ab}|^2\omega/3\hbar cKu$ is the linear gain at the line centre; $|d_{ab}|$ is the reduced matrix element of the dipole transition moment; $\gamma_{a,b}$ are the relaxation constants of the lower and upper levels, respectively; N is the population difference density; $I_{1k}^{\prime +} = (I_1^{\prime -}I_2^{\prime +}I_2^{\prime -}/I_1^{\prime +})^{1/2}$; $W(x \pm \Delta, y) = U(x \pm \Delta, y) + \mathrm{i}V(x \pm \Delta, y)$ is the complex error function; $\bar{W}_{1,2}^{\pm} = \bar{U}_{1,2}^{\pm} + \mathrm{i}\bar{V}_{1,2}^{\pm} = [W(x_{1,2}^{\pm} - \Delta, y) + W(x_{1,2}^{\pm} + \Delta, y)]/2$; $\Delta W_{1,2}^{\pm} = [W(x_{1,2}^{\pm} - \Delta, y) - W(x_{1,2}^{\pm} + \Delta, y)]/2$; $x_{1,2}^{\pm} \pm \Delta = (\omega_{1,2}^{\pm} - \omega_0 \pm g\mu_{\mathrm{B}}H)/Ku$ is the detuning of the laser frequency $\omega_{1,2}^{\pm}$ from the contour centre ω_0; $x' = xKu/2\pi$ (in hertz); $\Delta = g\mu_{\mathrm{B}}H/Ku$; g is the Lande factor; μ_{B} is the Bohr magneton; H is the longitudinal magnetic field strength in the medium; $Ku = \Delta\omega_{\mathrm{D}}/2 \times \sqrt{\ln 2}$; $\Delta\omega_{\mathrm{D}}$ is the Doppler contour width; $y = \gamma_{ab}/Ku$; and γ_{ab} is the homogeneous linewidth. The nonlinear self-action coefficients $c_1^{+\prime}$, $c_1^{+\prime\prime}$, the coefficients a_{11}^{+-} $(b, \tilde{b}, d)$, $a_{12}^{\pm\mp}$ $(b, \tilde{b}, d)$ of interaction of the wave 1^{+} with unidirectional and counterpropagating travelling waves, and the coefficients $a_{1k}^{+}, b_{1k}^{+}, \tilde{b}_{1k}^{+}, d_{1k}^{+}$, of combinational interaction contributing to the polarisability of the medium at the frequency ω_1^{+} for a single-isotopic gas in the Doppler limit and the approximation of relaxation constants $\gamma_a, \gamma_b, \gamma_{ab}$ are presented in Appendix. For arbitrary broadening, the equiisotopic composition, and taking into account the orienation and alignment constants, they can be obtained based on the results of papers [34, 37, 38]. The expression for the tensor $\hat{\chi}_1^{-}$ can be obtained from (9) by making the $+ \leftrightarrow -$ index replacement, and for the tensor $\hat{\chi}_2^{\pm}$ – from $\hat{\chi}_1^{\pm}$ by making the $1 \leftrightarrow 2$ replacement.

We will derive equations of motion (lasing is also possible) for the 1^{+} wave in the scalar form by using the equation

$$\hat{M}^{+}\boldsymbol{E}_{jM}^{+} = \lambda_{jM}^{+}\boldsymbol{E}_{jM}^{+}, \quad j = 1, 2 \tag{10}$$

for determining the polarisation–frequency characteristics of the cavity modes by neglecting backscattering. By transposing this equation, we multiply it from the right by the matrix

$$\begin{pmatrix} 0 & -1 \\ 1 & 0 \end{pmatrix},$$

and then multiply the obtained equality from the left by he nonstationary equation for the wave 1^{+} following from the system of vector equations (6). Hereafter, the subscript M is assigned to the eigenvalues and eigenvectors of the cavity matrix. Then, taking into account the relations

*A nonlinear medium can be considered homogeneous only approximately if the parameters of radiation propagating in it remain invariable and equal to the parameters of radiation incident on the medium, which is valid in the approximation of the third-order field perturbation theory.

$$\tilde{\hat{M}}\begin{pmatrix}0 & -1\\ 1 & 0\end{pmatrix}\hat{M}=\begin{pmatrix}0 & -1\\ 1 & 0\end{pmatrix}\det\hat{M},$$

$$\exp(h_1^+ + \hat{H}_1^+ + \ln\lambda_{1M}) \approx 1 + h_1^+ + \ln\lambda_{1M}^+ + \hat{H}_1^+, \quad (11)$$

$$\det\hat{M}^+ = \lambda_{1M}^+\lambda_{2M}^+,$$

we represent equations of the lasing of the wave 1^+ in the form

$$\cot(z_1^+ - z_{2M}^+)\frac{\mathrm{d}z_1^+}{\mathrm{d}t'} + \frac{\mathrm{d}}{\mathrm{d}t'}\left(\ln\sqrt{\frac{I_1^+}{\cosh\beta_1^+}} + \mathrm{i}\Psi_1^+\right)$$

$$= h_1^+ + \ln\lambda_{1M}^+ + r_1^-\frac{\sin(z_{2M}^+ - z_1^-)}{\sin(z_{2M}^+ - z_1^+)}\frac{\sqrt{I_1^-/\cosh 2\beta_1^-}\,\mathrm{e}^{\mathrm{i}\Psi_1^-}}{\sqrt{I_1^+/\cosh 2\beta_1^+}\,\mathrm{e}^{\mathrm{i}\Psi_1^+}}$$

$$+ \alpha t_2^+\frac{\sin(z_{2M}^+ - z_2^+)}{\sin(z_{2M}^+ - z_1^+)}\frac{\sqrt{I_2^+/\cosh 2\beta_2^+}\,\mathrm{e}^{\mathrm{i}\Psi_2^+}}{\sqrt{I_1^+/\cosh 2\beta_1^+}\,\mathrm{e}^{\mathrm{i}\Psi_1^+}}$$

$$+ (\cos z_{2M}^+, \sin z_{2M}^+)\begin{pmatrix}0 & -1\\ 1 & 0\end{pmatrix}\hat{H}_1^+\begin{pmatrix}\cos z_1^+\\ \sin z_1^+\end{pmatrix}$$

$$\times\left[\sin(z_{2M}^+ - z_1^+)\sqrt{I_1^+/\cosh 2\beta_1^+}\,\mathrm{e}^{\mathrm{i}\Psi_1^+}\right]^{-1}. \quad (12)$$

Equations (12) are written by assuming that the reflection and transmission coefficients for counterpropagating waves belonging to one cavity eigenvalue satisfy the conditions $|t| \approx 1$, $|r| \ll 1$, and the inverse scattering from one cavity mode to another is small ($|\alpha| \ll 1$), so that only the terms of the first-order smallness in r and α are taken into account in (12). The equations of lasing for the wave 1^- are obtained from (12) by the $+ \leftrightarrow -$ index replacement, and equations for the waves 2^+ (2^-) are obtained from equation for the waves 1^+ (1^-) by the $1 \leftrightarrow 2$ replacement.

In a strongly anisotropic-cavity gas laser, where the relaxation times of polarisation characteristics are much shorter than the relaxation times of the intensities and phases of generated waves, the time dependence of polarisation states can be neglected ($\mathrm{d}z/\mathrm{d}t' = 0$), by assuming that they are constant and equal to polarisation parameters specified by the cavity: $z_{1,2} = z_{1M,2M}$. As follows from (12), this allows one to neglect the influence of backscattering from one mode to another. In addition, expression (12) for a strongly anisotropic-cavity gas laser contains the phase difference of counterpropagating waves belonging to one cavity mode, which allows one to write equations for these variables, thereby reducing the dimensionality of the system.

Taking into account the explicit form of expressions for h_1^+ and $\hat{H}_1^+$, determined by (8) and (9), assuming that $t = 1$ and introducing the notation of experimentally measured quantities, we write the equations of lasing of the FRGL in the final form [41]

$$\frac{\mathrm{d}I_1^\pm}{\mathrm{d}\tau} = \left\{\frac{P_1^\pm}{P} - \mathrm{Re}\left(\theta_{11}^{\pm\pm}I_1^\pm + \theta_{11}^{\pm\mp}I_1^\mp + \theta_{12}^{\pm\pm}I_2^\pm\right.\right.$$

$$\left. + \theta_{12}^{\pm\mp}I_2^\mp + \theta_{1k}^\pm I_{1k} - R_1^\mp\sqrt{\frac{I_1^\mp}{I_1^\pm}}\mathrm{e}^{\mp\mathrm{i}\Psi_1}\right) -$$

$$\left. - \mathrm{Im}\left[\frac{\Delta W_1^\pm}{P}\cot(z_1^\pm - z_{2M}^\pm)\right]\right\}2I_1^\pm, \quad (13)$$

$$\frac{\mathrm{d}\Psi_1}{\mathrm{d}\tau} = \mathrm{Re}\left[\frac{\Delta W_1^+}{P}\cot(z_1^+ - z_{2M}^+) - \frac{\Delta W_1^-}{P}\cot(z_1^- - z_{2M}^-)\right]$$

$$+ \Delta\Omega_1 - \Delta\Omega_{10} + \frac{V_1^+ - V_1^-}{P} - \mathrm{Im}\left[\theta_{11}^{++}I_1^+ + \theta_{11}^{+-}I_1^-\right.$$

$$+ \theta_{12}^{++}I_2^+ + \theta_{12}^{+-}I_2^- + \theta_{1k}^+I_{1k}^+ - \theta_{11}^{--}I_1^- - \theta_{11}^{-+}I_1^+ - \theta_{12}^{-+}I_2^-$$

$$\left. - \theta_{12}^{+-}I_2^- - \theta_{1k}^-I_{1k}^- + R_1^-\sqrt{\frac{I_1^-}{I_1^+}}\mathrm{e}^{-\mathrm{i}\Psi_1} - R_1^+\sqrt{\frac{I_1^+}{I_1^-}}\mathrm{e}^{+\mathrm{i}\Psi_1}\right]. \quad (14)$$

Equations for $I_2^\pm$ and Ψ_2 are obtained from expressions (13) and (14) by the $1 \leftrightarrow 2$ replacement. Here, $I_{1,2}^\pm = I_{1,2}^{\prime\pm}/P$ are the dimensionless intensity of generated waves; $\Psi_{1,2}$ are the phase differences of counterpropagating waves belonging to one eigenvalue of the cavity matrix ($\Psi_1 = \Psi_1^+ - \Psi_1^-$, $\Psi_2 = \Psi_2^+ - \Psi_2^-$); $\Delta\Omega_{1,2}$ is the frequency difference of counterpropagating waves ($\Delta\Omega_1 = \Omega_1^+ - \Omega_1^-$, $\Delta\Omega_2 = \Omega_2^+ - \Omega_2^-$); $\Omega = \omega L/(c\tau_0)$; $\Delta\Omega_{10,20}$ is the frequency difference specified by the cavity ($\Delta\Omega_{10} = \Omega_{1\mathrm{c}}^+ - \Omega_{1\mathrm{c}}^-$, $\Delta\Omega_{20} = \Omega_{2\mathrm{c}}^+ - \Omega_{2\mathrm{c}}^-$); $\tau = t'\tau_0$; $\tau_0 = k_0 lP$; $P_{1,2}^\pm = \bar{U}_{1,2}^\pm - 1/\eta_{1,2}^\pm$; $P = \bar{U}|_{x=0} - (1/\eta_1^+ + 1/\eta_1^- + 1/\eta_2^+ + 1/\eta_2^-)/4$; and $\eta_{1,2}$ is the pump excess over the threshold at the line centre.

The self-saturation and cross-saturation coefficients have the form

$$\theta_{11}^{\pm\pm} = c_1'^\pm + \mathrm{i}c_1''^\pm\cot(z_1^\pm - z_{2M}^\pm), \quad (15)$$

$$\theta_{11}^{\pm\mp} = a_{11}^{\pm\mp} - \frac{b_{11}^{\pm\mp}\sin(z_1^\pm + z_{2M}^\pm) - \tilde{b}_{11}^{\pm\mp}\sin(z_1^\pm + z_{2M}^\pm)}{\cosh 2\beta_1^\mp\sin(z_1^\pm - z_{2M}^\pm)}$$

$$+ \mathrm{i}d_{11}^{\pm\mp}\cot(z_1^\pm - z_{2M}^\pm). \quad (16)$$

Expressions for $\theta_{12}^{\pm\pm}$ can be obtained from expressions for $\theta_{11}^{\pm\mp}$ by the formal $1^\mp \to 2^\pm$ index replacement at the parameters a, b, d, and $\cosh\beta$, and for $\theta_{12}^{\pm\mp}$ – by the $1^\mp \to 2^\mp$ replacement; the quantities $\theta_{1k}^\pm$ describing the combination interaction are obtained from expressions for $\theta_{11}^{\pm\mp}$ by the $1^\mp \to k$, $\cosh\beta_k = \cosh\beta_2^\pm$ replacement. Expressions for $\theta_{22}^{\pm\pm}$, $\theta_{22}^{\pm\mp}$, $\theta_{21}^{\pm\pm}$, $\theta_{21}^{\pm\mp}$, $\theta_{2k}^\pm$ follow from expression for $\theta_{11}^{\pm\pm}$, $\theta_{11}^{\pm\mp}$, $\theta_{12}^{\pm\pm}$, $\theta_{12}^{\pm\mp}$, $\theta_{1k}^\pm$ after the $1 \leftrightarrow 2$ replacement.

The backscattering coefficients depend on the polarisation of generated waves:

$$R_1^\mp = \frac{r_1^\mp}{\tau_0}\sqrt{\frac{\cosh 2\beta_1^\pm}{\cosh 2\beta_1^\mp}}\frac{\sin(z_{2M}^\pm - z_1^\mp)}{\sin(z_{2M}^\pm - z_1^\pm)},$$

$$R_2^\mp = \frac{r_2^\mp}{\tau_0}\sqrt{\frac{\cosh 2\beta_2^\pm}{\cosh 2\beta_2^\mp}}\frac{\sin(z_{1M}^\pm - z_2^\mp)}{\sin(z_{1M}^\pm - z_2^\pm)}. \quad (17)$$

Equations (13) and (14) are valid for the third-order field perturbation theory upon the adiabatic elimination of the dynamics of variables of the medium, for a longitudinal magnetic field applied to the medium, and for the cavity anisotropy of an arbitrary type greatly exceeding the medium anisotropy (a strongly anisotropic-cavity laser). So far backscattering has been taken into account only for counterpropagating waves with coinciding linear polarisation states (see, for example, [5]). Unlike previous FRGL

models (see, for example, [4–6]), this model also takes into account the deformation of the polarisation states of generated waves [42, 36] during their propagation in the active medium. In the case of the linear phase anisotropy of the cavity, all the lasing regimes observed in experiments [7] were obtained in [41] based on equations (13) and (14).

The main advantage of the model proposed in the paper is the explicit dependences of the backscattering coefficients on the polarisation states of generated waves, which allow one to study the influence of polarisation on the width of the frequency synchronisation zone of a laser gyro. It follows from (17) that the coefficients $R_{1,2}^{\mp}$ achieve maximum values in the case of linearly polarised counterpropagating waves and vanish in the case of circularly polarised waves. The nonzero width of the synchronisation zone in the case of circular polarisation can be caused by the depolarisation of radiation upon backscattering.

Consider a particular case of the generation of elliptically polarised waves, which are produced by placing a linear phase plate and an optical rotator into the FRGL cavity. The Jones matrices of such a cavity for counterpropagating waves ($\pm$) have the form

$$\hat{M}^{+} = \begin{pmatrix} \mathrm{e}^{\mathrm{i}\psi} & 0 \\ 0 & \mathrm{e}^{-\mathrm{i}\psi} \end{pmatrix} \begin{pmatrix} \cos\phi & -\sin\phi \\ \sin\phi & \cos\phi \end{pmatrix}, \hat{M}^{-} = \tilde{\hat{M}}^{+}, \quad (18)$$

where ψ and ϕ are the linear and circular phase anisotropy and tilde means transposition. The eigenvalues of matrices $\hat{M}^{\pm}$ and the frequency difference of unidirectional and counterpropagating waves are determined by the expressions

$$\lambda_{1M,2M}^{\pm} = \cos 2\psi \cos 2\phi \pm (\cos^2 2\psi \cos^2 2\phi - 1)^{1/2},$$
$$\omega_{\mathrm{c}1}^{\pm} - \omega_{\mathrm{c}2}^{\pm} = 2\arccos(\cos 2\psi \cos 2\phi)c/L, \quad (19)$$

and the polarisation states of cavity modes are described by the expressions [36]

$$\gamma_{1M}^{+} = 1/2 \arctan\{-\tan\phi\}, \quad \sinh 2\beta_{1M}^{+} = -\sin\phi \cot\psi,$$
$$\gamma_{1M}^{+} - \gamma_{2M}^{+} = \pi/2, \quad \xi_{2M}^{+} = -\xi_{1M}^{+}, \quad (20)$$
$$\gamma_{1M,2M}^{-} = \gamma_{1M,2M}^{+}, \quad \xi_{1M,2M}^{-} = -\xi_{1M,2M}^{+}.$$

It follows from (20) that the unidirectional waves are polarised orthogonally, while the counterpropagating waves belonging to the same eigenvalues of the cavity matrix are polarised nonorthogonally, their azimuths being the same and ellipticities having the opposite signs.

3. Self-oscillation lasing regimes

The four-frequency ring gas laser considered here has many experimentally controlled parameters. Therefore, by integrating numerically equations (13) and (14), we will determine first the region of values for the linear and circular phase anisotropy of the cavity in which self-oscillations regimes of lasing of elliptically polarised waves are possible. This region is shown in Fig. 2. One can see from the diagram that, self-oscillations in this system can occur if the ellipticity is not too large: $0 \leqslant \xi < 0.2$. The diagram was calculated for $\lambda = 1.15$ μm, $c/L = 417$ MHz, $Ku/2\pi = 480$ MHz, $\eta_1^{\pm} = \eta_2^{\pm} = 1.3$, $y = 0.178$, $y_1 = \gamma_a/2Ku = 0.014$, and $y_2 = \gamma_b/2Ku = 0.0215$, for the initial conditions $I_{1,2}^{\pm}|_{\tau=0} = 0$, and $\Psi_{1,2}|_{\tau=0} = 0$, and dissipative coupling $(\phi_{1,2}^{+} + \phi_{1,2}^{-})/2 = \pi/2$, as well as for $x = 0$ and $r_1^{\mp}/(\cosh 2\beta_1\tau_0) = r_2^{\mp}/(\cosh 2\beta_1\tau_0) = r = 0.001$. We used in calculations the nonlinear interaction coefficients c, a, b, and d for single-isotope gas in the Doppler limit in the approximation of three relaxation constants by neglecting the combination interaction.

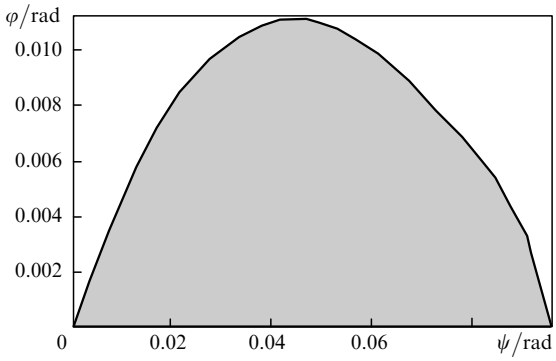

Figure 2. Self-oscillation region (grey) for $x = 0$, $r_{1,2}^{\pm} = 0.001$.

Consider now the influence of the amplitude of the backscattering coefficient and detuning of the lasing frequency from the gain line centre on the FRGL dynamics for different values of the linear and circular phase anisotropy from the self-oscillation region. For $\psi = 0.005$ rad, $\phi = 0.0015$ rad, which specify, according to (20), the polarisation–frequency characteristics of the cavity modes $\gamma_{1M}^{+} = -7.5 \times 10^{-4}$ rad, $\xi_{1M}^{+} = -0.146$ and $(\omega_{\mathrm{c}1} - \omega_{\mathrm{c}2})/2\pi = 1.38$ MHz, Fig. 3 presents the diagram of attractors (stable solutions of lasing equations) in the plane (r, x), calculated for the zero initial conditions $I_{1,2}^{\pm}|_{\tau=0} = 0$ and $\Psi_{1,2}|_{\tau=0} = 0$.

Note that, because the polarisation states of counterpropagating waves forming a standing wave are different, lasing regimes 2 and 3 in Fig. 3 can be only conditionally called standing-wave regimes because the counterpropagating components in the standing wave have the same polarisation.

Figure 4 shows periodic oscillations of the intensities $I_1^{\pm}$, $I_2^{\pm}$ and phase differences $\Psi_{1,2}$ for $r = 0.001$ for $I_{1,2}^{\pm}|_{\tau=0} = 0$ and $\Psi_{1,2}|_{\tau=0} = 0$ and different detunings from the line centre.

For the chosen cavity parameters, the FGRL dynamics with elliptically polarised waves demonstrates properties that are similar to those observed experimentally [7] and described theoretically [41] for linearly polarised waves. In both systems, the same lasing regimes exist: in the self-oscillation regime, the intensities $I_1^{\pm}$ ($I_2^{\pm}$) of counterpropagating waves belonging to the same eigenvalue of the cavity matrix, and the intensities I_1^{+}, I_2^{+} (I_1^{-}, I_2^{-}) of unidirectional waves oscillate out of phase, while the intensities I_1^{+}, I_2^{-} (I_1^{-}, I_2^{+}) of counterpropagating waves belonging to different eigenvalues of the cavity matrix oscillate in phase; the transition through the line centre is accompanied by the switching of intensities and polarisation states of counterpropagating and unidirectional waves.

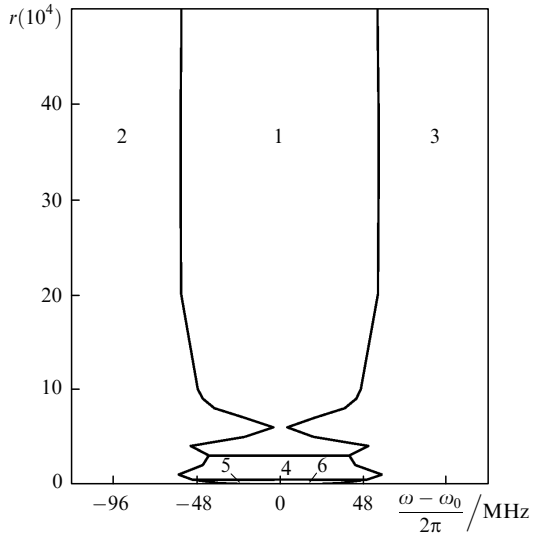

Figure 3. Diagram of attractors (stable solutions of the equations of lasing of a FRGL) for $\psi = 0.005$ rad, $\phi = 0.0015$ rad, $\gamma_{1M}^{+} = -7.5\times 10^{-4}$ rad, $-\xi_{1M}^{+} = 0.146$ and $(\omega_{c1} - \omega_{c2})/2\pi = 1.38$ MHz. Lasing regimes shown in the figure: (1) self-oscillations of the intensity $I_{1,2}^{\pm}$ of four travelling waves and the phase differences $\Psi_{1,2}$ of counterpropagating waves; (2) stationary regime of lasing of two counterpropagating waves 1^{+} and 1^{-} with identical intensities and frequencies, and the phase difference $\Psi_1 = -\pi/2$; (3) stationary single-frequency regime of lasing of a standing wave formed by two counterpropagating traveling waves 2^{+} and 2^{-} with the phase difference $\Psi_2 = \pi/2$; (4) stationary regime of lasing of four traveling waves with different intensities; (5, 6) stationary two-frequency regime of lasing of two orthogonal elliptically polarised counterpropagating waves $1^{+}, 2^{-}$ and $2^{+}, 1^{-}$, respectively, with different frequencies.

Figure 5 illustrates the behaviour of phase characteristics in the detuning region near the line centre, where the intensity switching takes place. One can see from Fig. 5a that the average values of the phase difference are constant ($\bar{\Psi}_1 = -\pi/2$, $\bar{\Psi}_2 = +\pi/2$) and do not change after passing through the line centre, experiencing jumps by 2π away from it. The instantaneous values of the phase difference change continuously (Fig. 5b) in the narrow detuning region (a few tens of kilohertz) near the point $x' \approx -125$ kHz rather than at the line centre. A similar behaviour of phase variables was found in the theoretical study [43] of the dynamics of a scalar field class B laser.

A specific feature of the generation of an electromagnetic wave with the nonzero ellipticity compared to a linearly polarised wave is the appearance of the additional phase shift described by the expression [39, 38]

$$\Psi_{\mathrm{p}} = \arctan(\xi \tan\gamma). \tag{21}$$

If the phase differences determined by the polarisation of cavity modes according to (20) are taken as the initial phase differences, the type of oscillations will considerably change. Figure 6 shows periodic oscillations of the intensity and phase difference of counterpropagating waves for $I_{1,2}^{\pm}|_{\tau=0} = 0$, $\Psi_1|_{\tau=0} = 2.2\times 10^{-4}$ rad, $\Psi_2|_{\tau=0} = -3.13$ rad, other parameters being as in Fig. 4. One can see that self-oscillations have the same form in a broad detuning range to the right and left of the centre as at the centre. The intensity switching occurs at detunings $x \approx \pm 36$ MHz symmetric with respect to the centre. The phase characteristics in the vicinity of switching points change as it occurs near the centre (Fig. 5).

The shift of the intensity switching in detuning caused by the phase shift of the wave, whose value is determined by the polarisation state of the wave, is the effect of the polarisation-phase dynamics. The appearance of the additional phase difference of generated waves, caused by the different

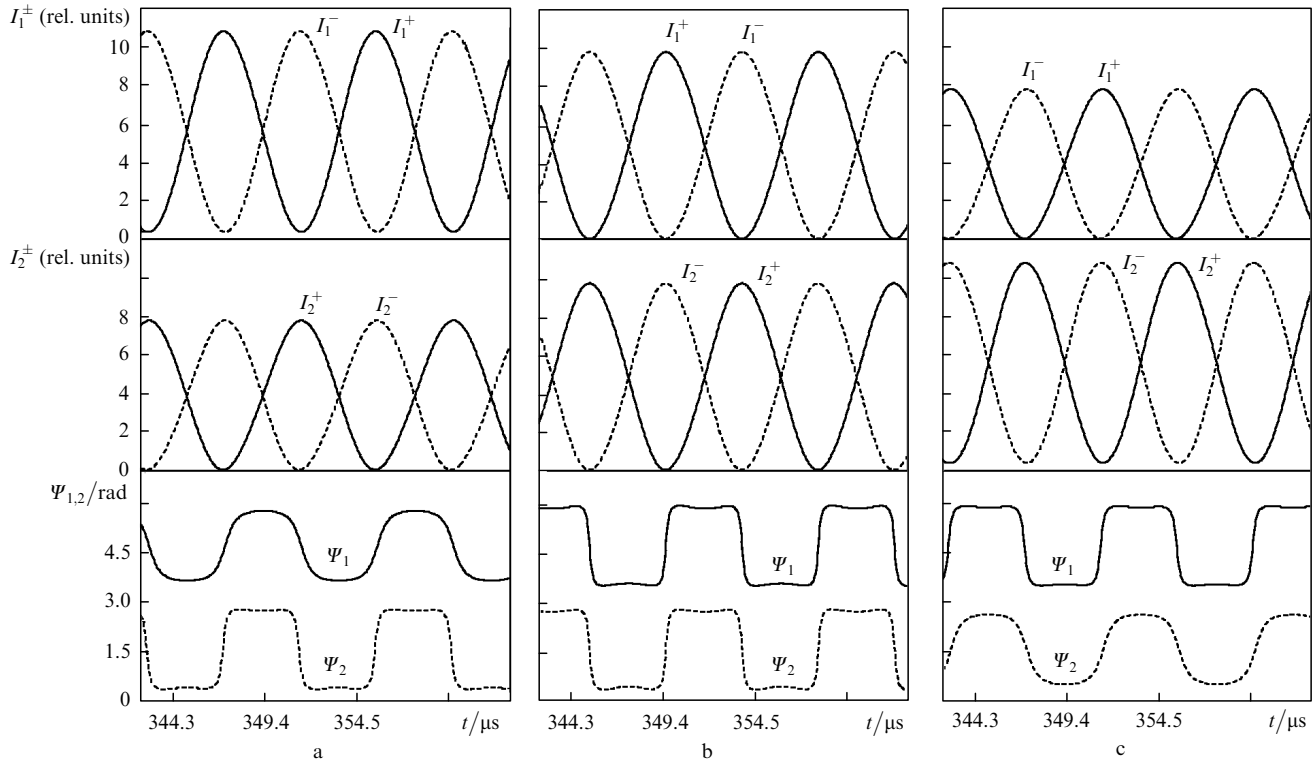

Figure 4. Self-oscillation lasing regimes for $x' = -43.2$ MHz (a), $x' = 0$ (b) and $x' = 43.2$ MHz (c) for $I_{1,2}^{\pm}|_{\tau=0} = \Psi_{1,2}|_{\tau=0} = 0$ and $r = 0.001$.

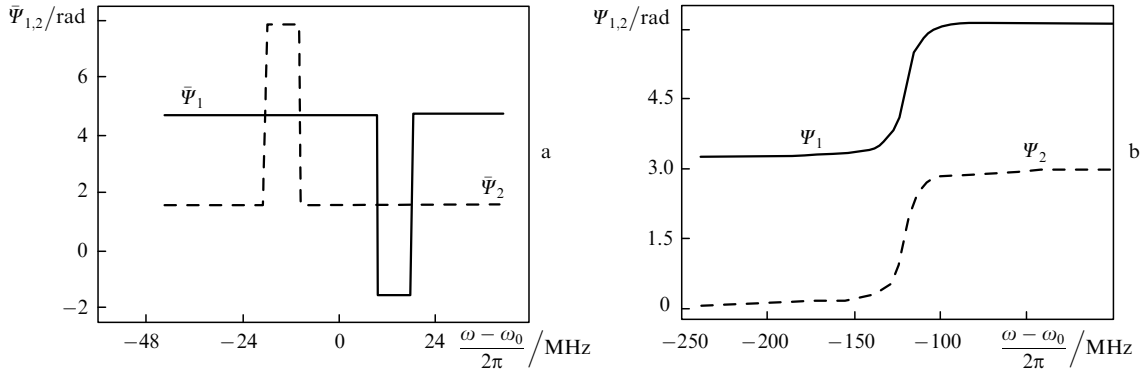

Figure 5. Dependences of the mean phase differences $\bar{\Psi}_1$, $\bar{\Psi}_2$ (a) and their instantaneous values (b) on detuning.

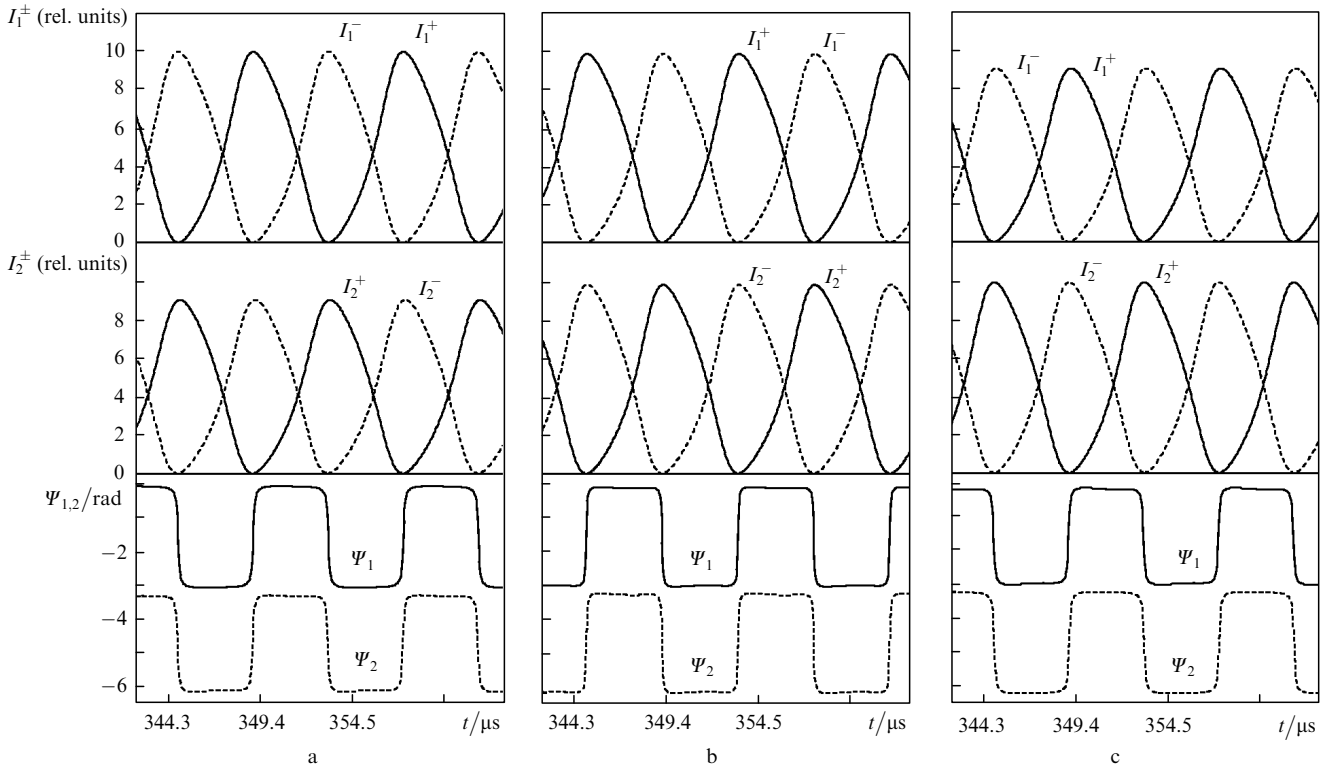

Figure 6. Same as in Fig. 5, but for $I_{1,2}^{\pm}|_{\tau=0} = 0$, $\Psi_1|_{\tau=0} = 2.2 \times 10^{-4}$ rad and $\Psi_2|_{\tau=0} = -3.13$ rad.

states of polarisations of these waves, and changing qualitatively the type of the system dynamics, was found in the description of the interference of two quasi-monochromatic waves [17]. Here, it is pertinent to recall the influence of polarisation on the frequency characteristics of ring gas lasers in the stationary regime, when the difference in ellipticities of counterpropagating waves in lasers gives rise to the difference in their frequencies, i.e. to the polarisation nonreciprocity [44, 35].

4. Chaotic and stochastic regimes

An understanding of the importance of chaotic and stochastic regimes in the functional processes of neural devices, biological, social, and economic systems, in the development of new principles of data processing, data security in optical communication devices, in the development of optical computers, etc. has made these regimes be the object of extensive recent investigations. At present there exist a number of scenarios of evolution from the stationary solution to the periodic one and, finally, to the chaotic solution (see, for example, [45–48]); however, the picture of the possible ways of the appearance and manifestations of chaos is far from complete. One of the problems being extensively studied in the last years is the appearance of chaos in nonlinear systems with symmetry (see, for example, [49, 50]). The symmetry of a dynamic system leads to the bistability and multistability of attractors with different topologies, resulting in the appearance of complicated regimes due to the interaction of chaotic attractors when the trajectory falls into the basin of attraction of two (or several) such attractors (see, for example, [47]) or due to the appearance of complex periodic solutions (with trajectories covering several stationary

states) evolving to a chaotic attractor with a complex topology upon changing the control parameter. One of the possible mechanisms of the appearance of complex dynamic structures is the influence of random fluctuations.

4.1 Spontaneous phase symmetry breaking and the deterministic chaos

The phenomena of the polarisation symmetry breaking and restoration were described with the help of singular (symmetric) bifurcations of stationary and periodic solutions in [51]. The consideration of the linear coupling of counterpropagating waves allows one to discover the effects of the phase symmetry breaking and restoration. The spontaneous phase symmetry breaking, defined as the passage from the self-oscillation regime with the zero frequency difference of counterpropagating waves to the bistable self-oscillation regime with the nonzero frequency difference of these waves, was discovered in a class A single-mode two-frequency laser with the coinciding linear polarisation states of the laser waves [52, 53].

In the absence of a longitudinal magnetic field on the active medium, equations of lasing (13) and (14) are invariant with respect to the transformations [54]

$$G = \{I_1^+, I_2^+, I_1^-, I_2^-, \Psi_1, \Psi_2, \Delta\Phi\}$$

$$\to \{I_1^-, I_2^-, I_1^+, I_2^+, , \Delta\Phi - \Psi_1, , \Delta\Phi - \Psi_2, , \Delta\Phi\}, \quad (22)$$

$$G = \{I_1^+, I_2^+, I_1^-, I_2^-, \Psi_1, \Psi_2, x\}$$

$$\to \{I_2^+, I_1^+, I_2^-, I_1^-, -\Psi_2, -\Psi_1, -x\}, \quad (23)$$

where $x = (x_1^+ + x_2^+)/2 = (x_1^- + x_2^-)/2$; and $\Delta\Phi = \phi_{1,2}^- - \phi_{1,2}^+$.

Condition (22) reflects the invariance of equations (13) and (14) with respect to the replacement of propagation directions under the condition of the constant phase difference, which for the equal intensities of travelling counterpropagating waves with identical frequencies represents the condition of formation of a standing wave, and for different intensities of these waves, leads to bistability. The second transformation depends on the detuning parameter, reflecting the invariance of the system with respect to the change of the sign of this parameter.

The invariance condition (22) is manifested in the appearance of periodic lasing regimes with different symmetry properties [55]: symmetric S cycles, whose trajectory in the phase space remains invariable after the transformation G, and asymmetric M cycles, which are always created in a pair and are transformed to each other by the transformation $GX_1(t) = X_2(t)$. The similarity of the symmetry properties of periodic lasing regimes and chiral and achiral biological macromolecules [56] makes it possible to use the dynamics of anisotropic laser systems for studying evolution processes in biology.

Figure 7 presents the diagram of attractors calculated in the plane (r, x) for $\psi = 0.08$ rad, $\phi = 0.07$ rad, $\gamma_{1M}^+ = -0.0035$ rad, $\xi_{1M}^+ = -0.0435$, $(\omega_{1c}^{\pm} - \omega_{2c}^{\pm})/2\pi = 21.3$ MHz, and the zero initial conditions. According to (23), in region 2 of stationary standing wave generation, for $x < 0$, the standing wave is formed by the counterpropagating travelling waves 1^+, 1^- with the phase difference $\Psi_1 = -\pi/2$, and for $x > 0$ – by the waves 2^+ and 2^- with the phase difference $\Psi_2 = \pi/2$. Figures 8a, b illustrate the behaviour of the average phase differences $\bar{\Psi}_1$ and $\bar{\Psi}_2$ for $r = 0.001$ and the zero initial conditions during the successive passing thorough regions $2 \to 1 \to 3 \to 1 \to 3 \to 1 \to 2$ from left to right (Fig. 7).

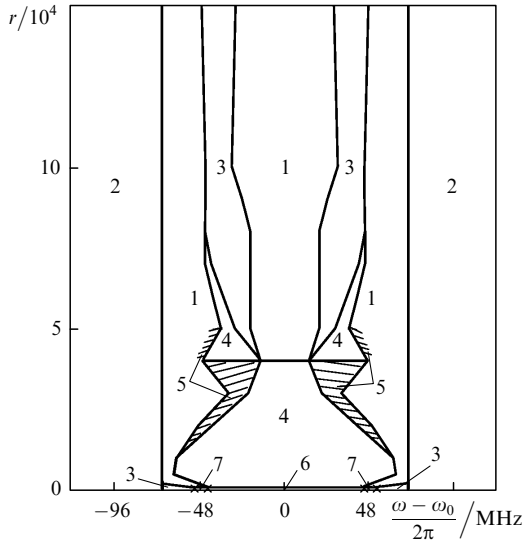

Figure 7. Diagram of attractors for $\psi = 0.08$ rad, $\phi = 0.07$ rad, $\gamma_{1M}^+ = -0.003$ rad, $\xi_{1M}^+ = -0.0435$ and $(\omega_{1c}^{\pm} - \omega_{2c}^{\pm})/2\pi = 21.3$ MHz. Lasing regimes shown in the figure: (1) self-oscillation regime corresponding to the symmetric limit cycle with out-of-phase oscillations of the intensities of counterpropagating waves with elliptic nonorthogonal polarisation states; (2) single-frequency stationary regime of lasing of a standing wave formed by two counterpropagating travelling waves with elliptical nonorthogonal polarisation states; (3) stationary regime of lasing of two standing waves with different intensities; (4) stationary regime of lasing of four travelling waves with different intensities; (5) asymmetric limit cycle and deterministic chaos; (6) stationary regime of lasing of two travelling waves with different intensities and frequencies ($1^+, 2^-$ to the left of the centre and $2^+, 1^-$ to the right of the centre); (7) asymmetric limit cycle of the second kind with the intensity oscillation and phase-difference rotation; lasing regimes caused by the sensitivity of the system to the action of random noise are shown by crosses.

One can see that these quantities change in the self-oscillation region due to jumps in the instantaneous phase differences by 2π, which do not change the intensity. The behaviour of the instantaneous intensities and phase differences is shown in Figs 8c, d. Depending on the detection conditions, for which a finite time interval was chosen, the average phase difference can change both continuously and jump-wise.

The transition from the regime 4 of lasing of four travelling waves to the regime 3 of lasing of two standing waves (both to the right and left of the line centre) is accompanied by the pitchfork bifurcation of the stationary solution. According to (22), for the specified value of the parameter Φ, the choice of one of the two possible solutions of the travelling wave type will be completely determined by fluctuations of the initial conditions, which suggest that the spontaneous phase symmetry breaking (restoration) takes place at the bifurcation point.

At the boundary of region 4, with increasing $|x|$ and constant r an asymmetric limit cycle appears due to the supercritical Hopf bifurcation from the stationary solution corresponding to the generation of four travelling waves. As

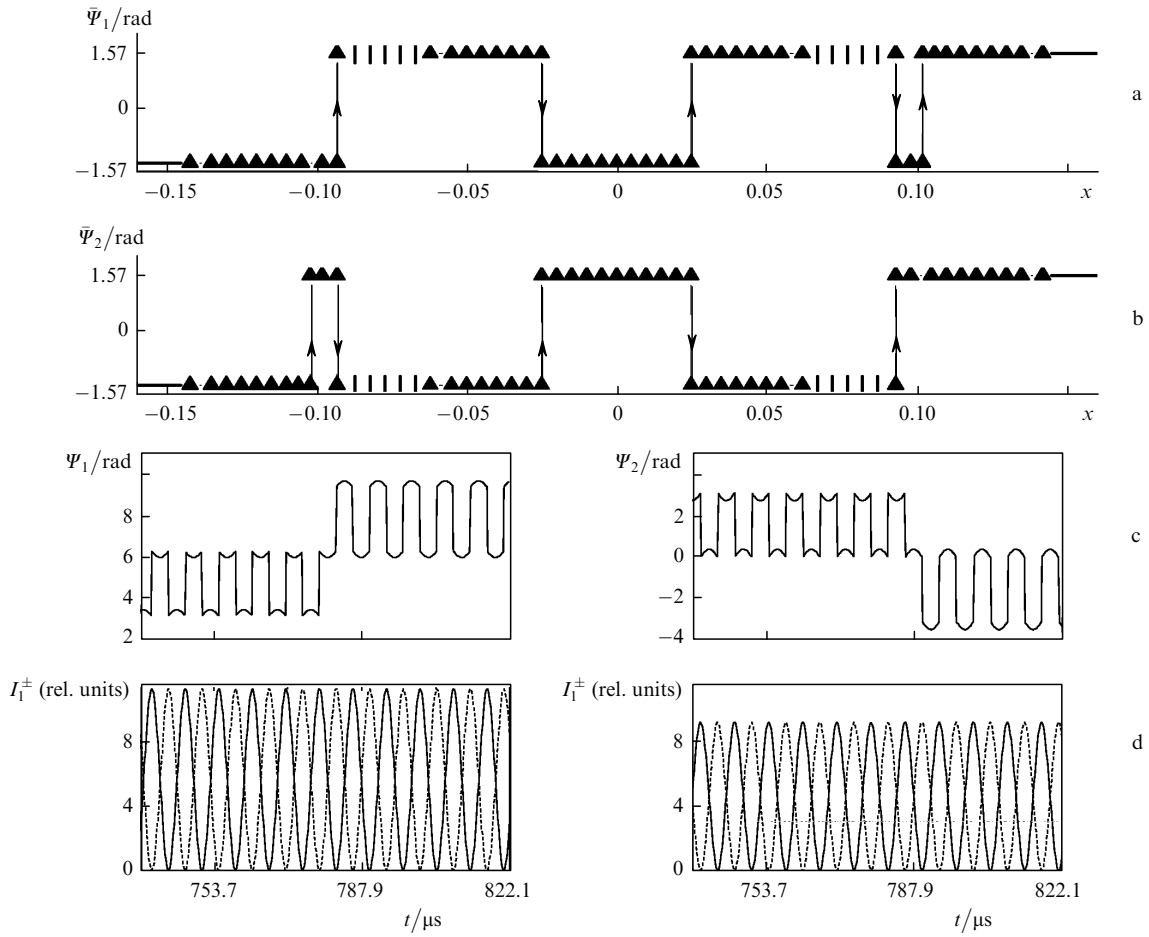

Figure 8. Changes in the mean phase differences $\bar{\Psi}_1$ (a) and $\bar{\Psi}_2$ (b) during moving from the region of negative detunings to the region of positive detunings, and jumps of the instant phase differences by 2π at invariable intensities; $x = -0.0235$ (c) and -0.0287 (d) ($I_{1,2}^{+}$ are shown by solid curves and $I_{1,2}^{-}$ – by dashed curves). The solid lines in Figures a, b correspond to stationary regime 2 of generation of one standing wave; vertical bars correspond to regime 3 of generation of two standing waves; triangles correspond to self-oscillation regime 1; the arrows show the directions of changing the mean phase differences by π.

$|x|$ is further increased in hatched region 5 (Fig. 7), depending on the value of the backscattering coefficient the M cycle behaves differently. Figure 9 illustrates the evolution of the phase trajectories and time realisations for $I_1^{\pm}$ and of the power spectra with increasing detuning x for $r = 0.0005$, beginning with the moment of appearance of the asymmetric limit cycle and ending by the appearance of the symmetric cycle (from top to bottom in Fig. 9). The numerical calculations were performed by using a sufficiently small step over the parameter. One can see that first, for $x' = -36$ MHz, the M cycle with the period T appears, which experiences two doubling-period bifurcations at $x' = -37.2$ and -38.2 MHz. Then, for $x' = -38.9$ MHz, the asymmetric double-band strange attractor is realised (see, for example, [45]) followed by a reverse period of doubling bifurcation cascade: the $4T$ cycle for $x' = -39.94$ MHz and the $2T$ cycle for $x' = -39.96$ MHz. Finally, for $x' = -39.97$ MHz, due to the pitchfork bifurcation of the periodic solution, the stable symmetric S cycle appears, i.e. the phase symmetry is restored (when the parameter is changed in the opposite direction, the phase symmetry is broken).

In region 1 (Fig. 7), the intensities and phase differences oscillate periodically with respect to the stationary solution corresponding to the regime of lasing of two standing waves. Therefore, we can assert that the spontaneous phase symmetry breaking in the FRGL under study, which is described by the pitchfork bifurcation, takes place both for the periodic and stationary solution in passing from the generation of travelling waves to the generation of standing waves.

The pitchfork bifurcation of the periodic solution accompanied by the appearance of chaos due to the Feugenbaum sequence was observed in a radio engineering system [57]; in laser and optical systems, it is found for the first time.

In region 5, where the deterministic chaos exists, depending on the initial conditions, attractors with different topologies can exist simultaneously (multistability). Thus, at the point $x' = -39.84$ MHz, $r = 0.0005$ for the zero initial conditions, the symmetric limit cycle is observed; when moving with a small step over the detuning parameter, the asymmetric strange attractor (similar to that presented in Fig. 9) is observed, while for the initial conditions $I_1^{+}|_{\tau=0} = 2.58, I_1^{-}|_{\tau=0} = 10.28, I_2^{+}|_{\tau=0} = 4.098, I_2^{-}|_{\tau=0} = 2.68$, $\Psi_1|_{\tau=0} = 0.947$ rad, and $\Psi_2|_{\tau=0} = -1.58$ rad, chaos can appear due to the bistability of asymmetric strange attractors: the system falls into tha basin of attraction of both attractors and is alternatively on one or the other. Figure 10 presents the phase projections, time realisations, and power spectra characterising the topology of such an asymmetric attractor. The experimental realisation of one of the possible

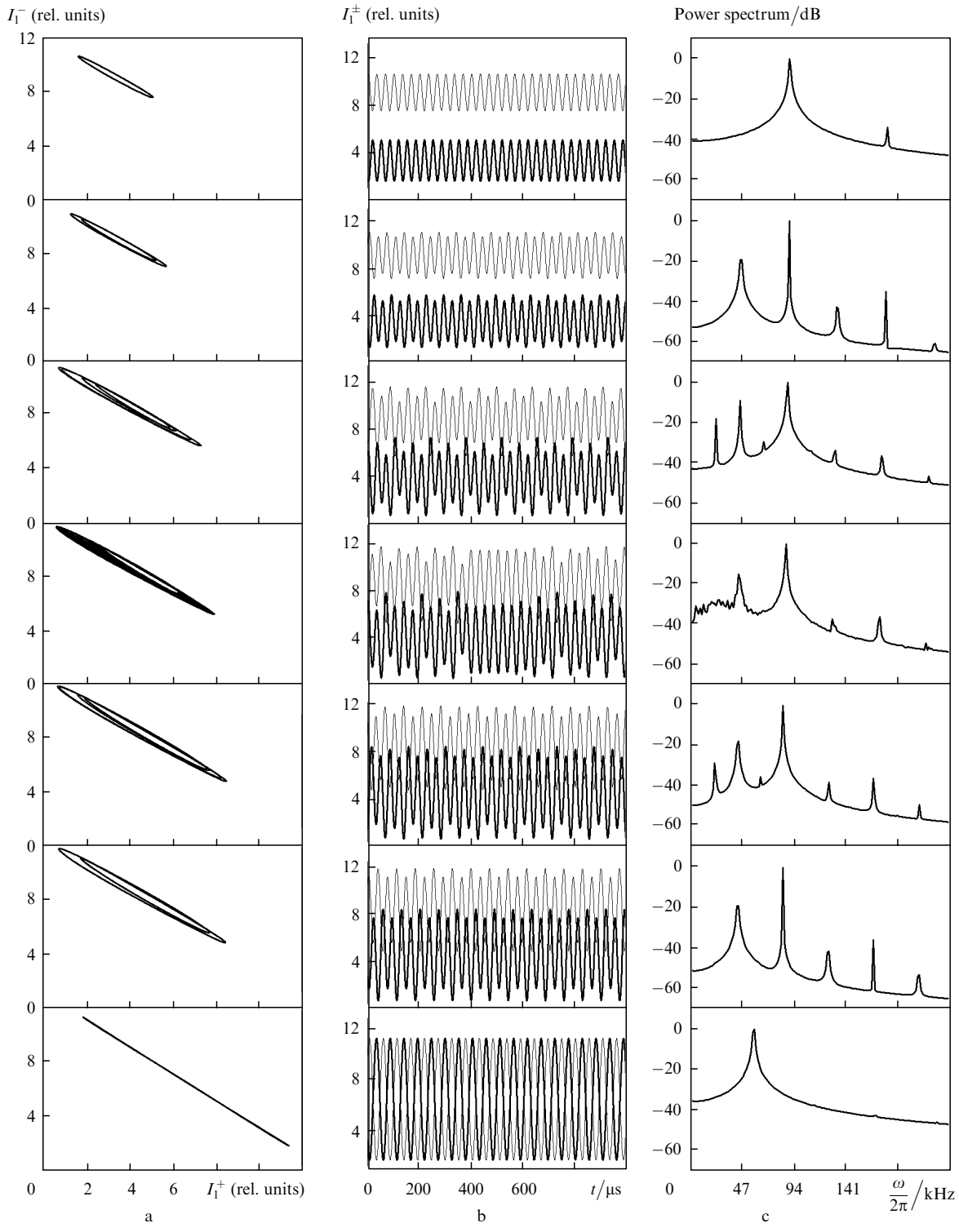

Figure 9. Evolution of the phase projections (a) and time realisations (b) for $I_1^{\pm}$, and of power spectra (c) for $r = 0.0005$; from top to bottom: the M cycles with periods T, $2T$, and $4T$; the asymmetric double-band strange attractor; the M cycles with periods $4T$ and $2T$; the S cycle.

regimes of lasing in the multistability region will depend on the properties of the FGGL under study and the scan rate of a measuring system during detuning.

4.2 Complicated noise-induced oscillations

Complicated noise-induced oscillations were observed in lasers with different active media: a gas laser [58], a semiconductor injection laser [59], and a vertical-cavity surface-emitting laser [60]. The influence of the rate of passing through a bifurcation point upon the symmetry breaking and the possibility of the predictable choice of one of the bistable solutions were studied theoretically in [61, 62].

The operation regimes of the FRGL sensitive to random perturbations appear at small backscattering coefficients in region 7 in the diagram of attractors (Fig. 7). Here, near the

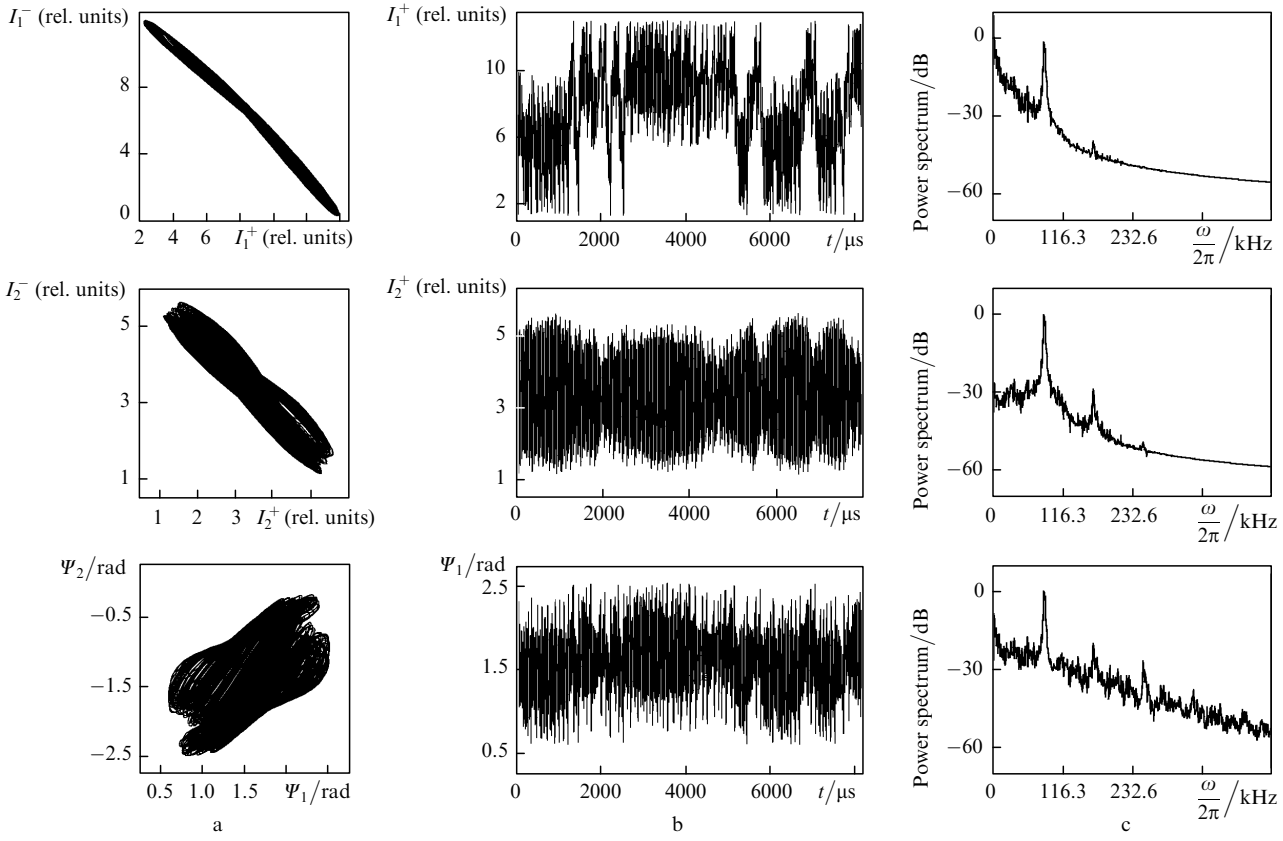

Figure 10. Strange attractor appearing due to the interaction of two asymmetric attractors; phase projections (a), time realisations (b), and power spectra (c) for I_1^+, I_2^+ and Ψ_1.

boundary with the stationary regime of lasing of travelling waves for $x' = -45.84$ MHz, an asymmetric limit cycle of the second kind is observed with the rotation of the phase difference Ψ_2 and oscillations of the wave intensity I_2^- near zero, which makes the system sensitive to random fluctuations, of different physical origins.

We will study the influence of random fluctuations by analysing the solutions of lasing equations (13) and (14) [63] written in the Langevin form with the additive inclusion of a random perturbation (see, for example, [64]); this is admissible under the condition that the intensity of random perturbations is low and is independent of variables and time.

To determine principal effects caused by low-intensity fluctuation perturbations, we consider, without specifying the physical nature of these perturbations, the influence of the delta-correlated (white) noise with the zero mathematical expectation and very low intensity, which can be conditionally treated as a weak perturbation of the trajectory of the system in the phase space. The sources of random fluctuations in the case of the white noise with the intensity D identical for all variables are defined as $\langle\xi(\tau)\rangle\langle\xi(\tau')\rangle = D\delta(\tau - \tau')$ (see, for example, [64]).

This consideration does not pretend to the mathematically correct description of the influence of random fluctuations, both external (thermal, etc.) and internal (spontaneous emission noise), which is rather complicated in the case of four-wave lasing. Nevertheless, it allows us to conclude that a mechanism of the development of complicated oscillations can exist in multimode laser systems, which is based on the stochastisation of the periodic regime with the oscillations of the intensity of one of the waves near the threshold.

Let us follow the evolution of the asymmetric limit cycle of the second kind with the lasing frequency detuning from the line centre in the presence of noise of intensity $D = 10^{-7}$. Figure 11 presents the time realisations and power spectra for the intensities $I_2^{\pm}$ for $x' = -45.84$ (a), -47.04 (b), -47.42 (c) and -48.47 MHz (d). The variable Ψ_2 behaves with respect to noise as I_2^-, while $I_1^{\pm}$ and Ψ_1 behave as I_2^+.

One can see that first the presence of noise affects only I_2^- (Fig. 11a), weakly distorting the time dependence and power spectrum in the high-frequency region of this variable. Then, the oscillation amplitude I_2^- increases due to nonlinear interaction, resulting in the increase in the amplitude of the high-frequency (noise) component in the power spectrum (Fig. 11b). In this case, other variables still remain insensitive to the perturbations of the system due to the complication of I_2^- oscillations. The estimate of the Lyapunov dimensionality of this attractor gives $\tilde{D} = 2.3$. As $|x|$ is increased, the oscillation amplitude I_2^- further grows, so that, by preserving the complicated shape, the amplitude becomes insensitive to the action of weak noise. The attractor dimensionality decreases to $\tilde{D} = 2.01$. However, due to rather large oscillation amplitude of 'noisy' variables, all variables of the system take the complex oscillation shape (Fig. 11c). And, finally, for $x' = -48.47$ MHz, the motion of the system becomes periodic with a very large period and complicated oscillation shape (Fig. 11d). Not performing quantitative studies of the degree of stochasticity (see, for example, [60]), we will assign conditionally complicated oscillations with a fractional dimensionality, existing in

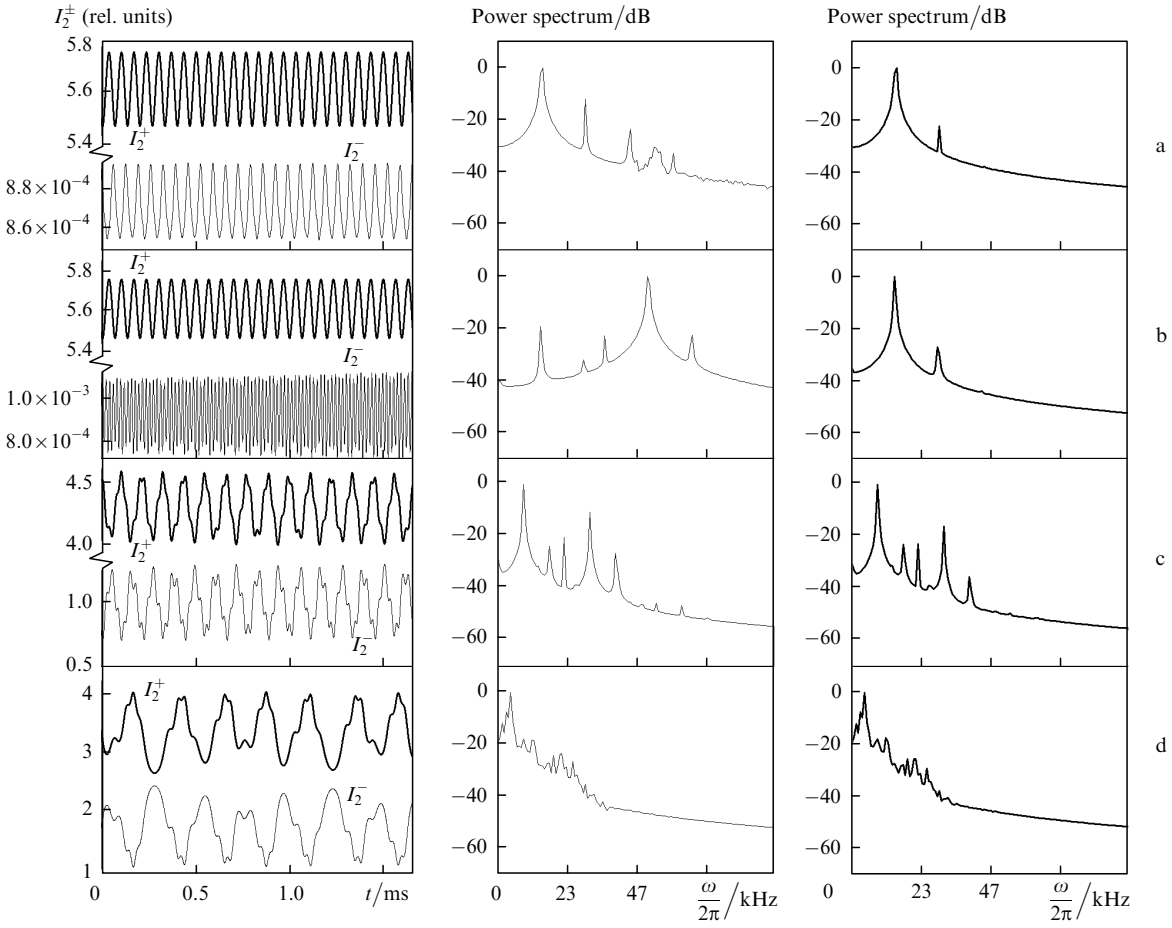

Figure 11. Evolution of the time realisations of the intensity $I_2^{\pm}$ and power spectra for I_2^- (middle column) and I_2^+ (right column): the limit cycle of the second kind in the presence of weak perturbations (a), stochastic oscillations (b), asymmetric chaos (c), and asymmetric limit cycle with the complicated shape of oscillations (d).

the region of the system sensitivity to noise, to stochastic oscillations (Fig. 11b), and oscillations with a fractional dimensionality in the region insensitive to noise (Fig. 11c) – to chaotic oscillations.

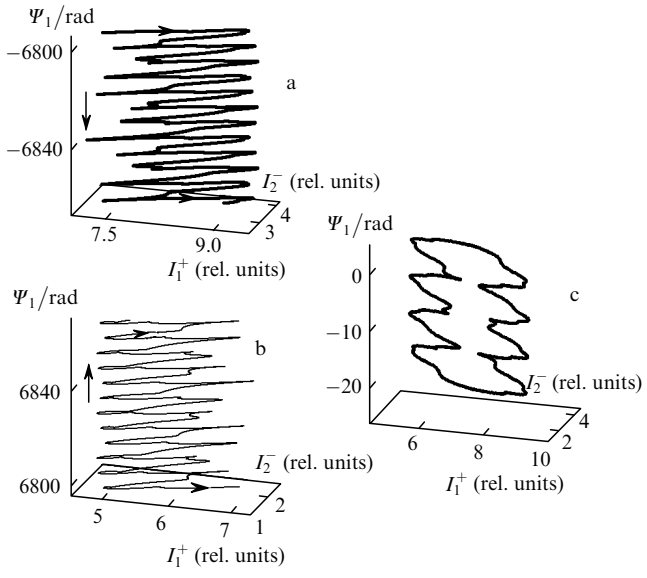

Figure 12. Spontaneous phase symmetry breaking (restoration) in three-dimensional projections for $r = 0.00001$; M cycles for $x' = -48.47$ (a, b) and the S cycle for $x' = -48.5$ MHz (c).

Then, for $x' = -48.5$ MHz, a pitchfork bifurcation occurs, resulting in the merging and disappearance of two long-period asymmetric limit cycles of the second kind and in the appearance of a long-period symmetric limit cycle of the first kind with the complicated oscillation shape. Figure 12 illustrates the phase symmetry restoration (breaking) for three-dimensional projections. Because the system at the bifurcation point is already insensitive to noise, we can assert that the choice of one of the asymmetric limit cycles is completely determined by the values of variables at the initial instant of time, which corresponds to the spontaneous phase symmetry breaking.

The evolution of the time realisations of $I_1^{\pm}$ for symmetric attractors with increasing detuning is shown in Fig. 13. Upon moving from top to bottom, for $x' = -47.8$ MHz (a), a symmetric limit cycle is fixed with the simplified oscillation shape and reduced period. Then, this cycle loses its stability, and symmetric chaos appears after the alternation, which exists for $x' = -49.4$ (b), -50.4 (c), -51.4 MHz (d), which is followed by the stationary regime of lasing of two standing waves with different intensities.

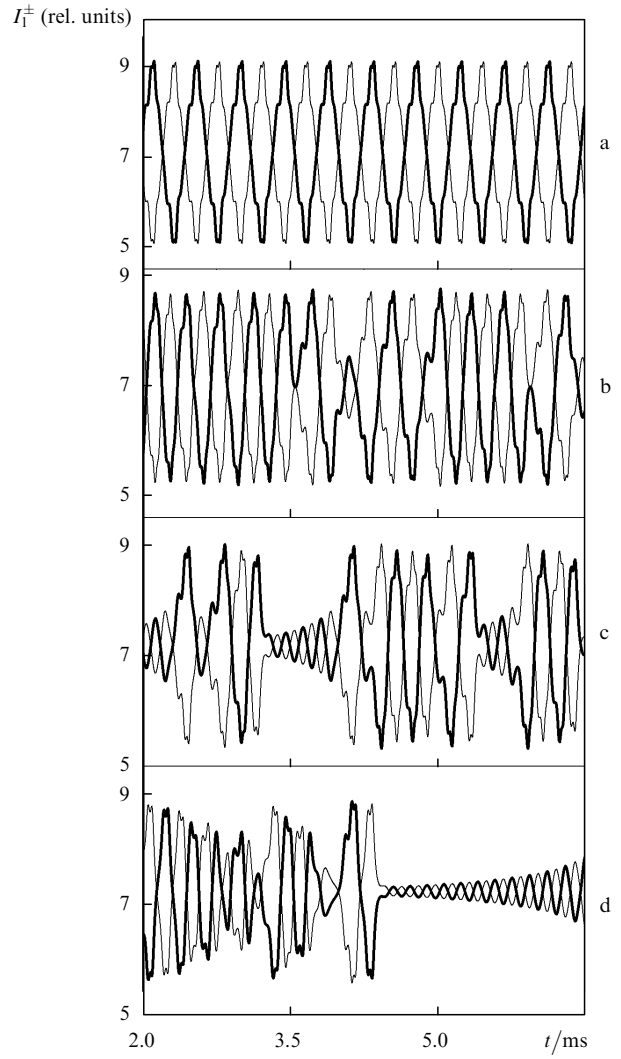

Figure 13. Evolution of the time realisations of the intensity $I_1^{\pm}$ of counterpropagating waves for the symmetric solution: the limit cycle (a), chaos (b – d) [I_1^+ (heavy curves), I_1^- (thin curves)].

5. Conclusions

The nonlinear dynamics caused by the instability of phase characteristics of the field generated in a FRGL with linearly coupled elliptically polarised waves has been studied by using the developed and experimentally tested model.

It has been shown the intensities, polarisation states, and phase differences of generated waves can be switched in the self-oscillation regime existing in a broad range of control parameters. The wave phase shift caused by the appearance of the nonzero ellipticity leads to the shift of the intensity switching from the detuning region near the gain contour centre (which is typical for linear polarisation) to the contour wing.

The symmetry properties of equations of lasing have been established. It has been shown that the spontaneous phase symmetry breaking for stationary and periodic solutions occurs upon transition from the regime of lasing of travelling waves to that of standing waves, which is achieved by detuning the lasing frequency from the line centre. Depending on the value of the backscattering coefficient in periodic regimes, both the deterministic and noise-induce chaos can appear in this case. The symmetry of the system causes the multistability of regular and chaotic attractors with different topologies.

A new mechanism of the appearance of complicated (chaotic and stochastic) oscillations in anisotropic lasers with the linear coupling has been discovered which consists in the stochastisation of periodic regimes with the intensity oscillations of one of the waves near the lasing threshold. Upon detuning in the presence of the delta-correlated white noise, these regimes give rise to stochastic oscillations and chaos with different symmetry properties. A FRGL with elliptically polarised waves can exhibit the following regimes with the complex dynamic structure: asymmetric chaos (appearing in the course of three different scenarios: the period doubling bifurcations cascade of the asymmetric limit cycle, the interaction of two asymmetric Feugenbaum attractors, and the stochastisation of the limit cycle of the second kind), noise-induced stochastic oscillations, and symmetric chaos appearing through the loss of the stability of the symmetric limit cycle and alternation.

The results of studying the dynamics of an anisotropic FGRL with symmetry can be used in informatics for the development of devices for data coding and protection, in biology for explaining mechanisms of the appearance of the chiral and achiral symmetry in nature, as well as for explaining the formation of dynamic structures in multi-dimensional coupled systems of different physical nature, in particular, multimode anisotropic lasers with more complex active media, which have not been theoretically described so far.

The FRGL model developed in this paper can be used in laser gyros for studying the dependence of the synchronisation zone width on the polarisation state of generated waves and investigating the polarisation nonreciprocity appearing due to defects in the manufacturing of cavity elements, the deformation of polarisation specified by the cavity in the active medium, and due to the depolarisation of back-scattered radiation. The consideration of a longitudinal magnetic field applied to the medium allows one to study magnetooptical effects.

Acknowledgements. This work was partially supported by the Belarusian Republican Foundation for Fundamental Research (Project No. F05-226).

Appendix

The nonlinear interaction coefficients in a FRGL for wave 1 corresponding to wave 1^+ ($2 \to 1^-$, $3 \to 2^+$, $4 \to 2^-$) in the presence of a longitudinal magnetic field in the active medium in the approximation of three relaxation constants ($y_{1,2} = \gamma_{a,b}/2Ku$, $y = \gamma/Ku$) and the limiting Doppler broadening have the form [38]

$$c_1' = \frac{\exp[-(x_1^2 + \Delta^2)]}{\cosh 2\beta_1} \times \left[R_1 \frac{y_1 + y_2}{y} \cosh 2(x_1\Delta + \beta_1) + C_1 + C_2 \right], \qquad \text{(A1)}$$

$$c_1'' = \frac{\exp[-(x_1^2 + \Delta^2)]}{\cosh 2\beta_1} \left[R_1 \frac{y_1 + y_2}{y} \times \right.$$

$$\times \sinh 2(x_1\Delta+\beta_1)+C_1C_2\Big], \tag{A2}$$

$$C_{1,2}=\frac{\exp[\pm 2(x_1\Delta-\beta_1)]}{2(y\mp\Delta)}\Big[R_2y_2+R_3y_1$$

$$+y_1y_2\left(\frac{R_3}{y_1\mp \mathrm{i}\Delta}+\frac{R_2}{y_2\mp \mathrm{i}\Delta}\right)\Big], \tag{A3}$$

$$a_{12}=\frac{\exp[-(x_1^2+\Delta^2)]}{\cosh 2\beta_1}[A_1\cosh 2(x_1\Delta+\beta_2)+A_2+A_3], \tag{A4}$$

$$A_1=\frac{R_1}{y+\mathrm{i}\Delta x_{12}}\Big[(y_1+y_2)+y_1y_2$$

$$\times\left(\frac{1}{y_1+\mathrm{i}\Delta x_{12}}+\frac{1}{y_2+\mathrm{i}\Delta x_{12}}\right)\Big], \tag{A5}$$

$$A_{2,3}=\frac{\exp[\pm 2(x_1\Delta-\beta_2)]}{2[y+\mathrm{i}(\Delta x_{12}\mp\Delta)]}\Big\{R_3y_1+R_2y_2+y_1y_2$$

$$\times\left[\frac{R_3}{y_1+\mathrm{i}(\Delta x_{12}\mp\Delta)}+\frac{R_2}{y_2+\mathrm{i}(\Delta x_{12}\mp\Delta)}\right]\Big\}, \tag{A6}$$

$$a_{13}=\frac{\exp[-(x_1^2+\Delta^2)]}{\cosh 2\beta_3}\Big\{\frac{\cosh 2(x_1\Delta-\beta_3)}{y+\mathrm{i}x_{13}}$$

$$\times(R_3y_1+R_2y_2)+\frac{R_1}{2}(y_1+y_2)\left[\frac{\exp 2(x_1\Delta+\beta_3)}{y+\mathrm{i}(x_{13}-\Delta)}\right.$$

$$\left.+\frac{\exp[-2(x_1\Delta+\beta_3)]}{y+\mathrm{i}(x_{13}+\Delta)}\right]\Big\}, \tag{A7}$$

$$b_{12},\tilde{b}_{12}=\frac{1}{2}\exp[-(x_1^2+\Delta^2)]y_1y_2(B_{10}\pm B_{20}), \tag{A8}$$

$$B_{10,20}=\frac{\exp[\pm 2(x_1\Delta-\mathrm{i}\gamma_2)]}{y+\mathrm{i}(\Delta x_{12}\mp\Delta)}\left(\frac{R_2}{y_1+\mathrm{i}\Delta x_{12}}\right.$$

$$\left.+\frac{R_3}{y_2+\mathrm{i}\Delta x_{12}}+\frac{R_3}{y_1\mp\mathrm{i}\Delta}+\frac{R_2}{y_2\mp\mathrm{i}\Delta}\right), \tag{A9}$$

$$b_{13},\tilde{b}_{13}=\frac{1}{2}\exp[-(x_1^2+\Delta^2)]y_1y_2(B_{13}\pm B_{23}),$$

$$B_{13,23}=\frac{\exp[\pm 2(x_1\Delta-\mathrm{i}\gamma_3)]}{y+\mathrm{i}(x_{13}\mp\Delta)}\left(\frac{R_3}{y_1\mp\mathrm{i}\Delta}+\frac{R_2}{y_2\mp\mathrm{i}\Delta}\right), \tag{A10}$$

$$d_{12}=\frac{\exp[-(x_1^2+\Delta^2)]}{\cosh 2\beta_2}[A_1\sinh 2(x_1\Delta+\beta_2)+A_2-A_3], \tag{A11}$$

$$d_{13}=\frac{\exp[-(x_1^2+\Delta^2)]}{\cosh 2\beta_3}\Big\{\frac{\sinh 2(x_1\Delta-\beta_3)}{y+\mathrm{i}x_{13}}$$

$$\times(R_3y_1+R_2y_2)+\frac{R_1}{2}(y_1+y_2)\left[\frac{\exp 2(x_1\Delta+\beta_3)}{y+\mathrm{i}(x_{13}-\Delta)}\right.$$

$$\left.-\frac{\exp[-2(x_1\Delta+\beta_3)]}{y+\mathrm{i}(x_{13}+\Delta)}\right]\Big\}, \tag{A12}$$

$$a_{1k},d_{1k}=\Big\{\frac{\alpha_1}{2}\frac{y_1y_2}{\cosh 2\beta_2}\left(\frac{1}{y_1+\mathrm{i}\Delta x_{12}}+\frac{1}{y_2+\mathrm{i}\Delta x_{12}}\right)$$

$$\times\left[\frac{\exp(z_1-z_3-z_2+z_4^*+2\mathrm{i}\delta_1\Delta)}{y+\mathrm{i}(\delta_1-\Delta)}\right.$$

$$\left.\pm\frac{\exp[-(z_1-z_3-z_2+z_4^*+2\mathrm{i}\delta_1\Delta)]}{y+\mathrm{i}(\delta_1+\Delta)}\right]$$

$$+\frac{\exp(z_1-z_3+z_2-z_4^*+2\mathrm{i}\delta_1\Delta)}{y+\mathrm{i}(\delta_1-\Delta)}$$

$$\times\left[\frac{R_3}{y_1+\mathrm{i}(\Delta x_{12}-\Delta)}+\frac{R_2}{y_2+\mathrm{i}(\Delta x_{12}-\Delta)}\right]$$

$$\pm\frac{\exp[-(z_1-z_3+z_2-z_4^*+2\mathrm{i}\delta_1\Delta)]}{y+\mathrm{i}(\delta_1+\Delta)}$$

$$\times\left[\frac{R_3}{y_1+\mathrm{i}(\Delta x_{12}+\Delta)}+\frac{R_2}{y_2+\mathrm{i}(\Delta x_{12}+\Delta)}\right]\Big\}, \tag{A13}$$

$$b_{1k}=b_0\cos 2\Psi_{1k},\ \tilde{b}_{1k}=-b_0\sin 2\Psi_{1k}, \tag{A14}$$

$$b_0=\alpha_1y_1y_2\frac{1}{y+\mathrm{i}\delta_1}\left(\frac{R_2}{y_1+\mathrm{i}\Delta x_{12}}+\frac{R_2}{y_1+\mathrm{i}\Delta x_{12}}\right),$$

$$\Psi_{1k}=z_3-z_2-z_1^*+\mathrm{i}\frac{2\delta_1\Delta}{Ku^2}, \tag{A15}$$

$$\alpha_1=N_{12}\exp[2\mathrm{i}(\Delta x_{13}-\Delta x_{24})]$$

$$\times\exp[-(\delta_1^2+\Delta^2)]\sqrt{\frac{\cosh 2\beta_1\cosh 2\beta_2}{\cosh 2\beta_3\cosh 2\beta_4}}, \tag{A16}$$

$$x_{ij}=(x_i+x_j)/2,\ \Delta x_{ij}=(x_ix_j)/2,\ \delta_1=x_1+\Delta x_{42}. \tag{A17}$$

The functions of the angular momenta R_1, R_2, R_3 of the working levels of atoms

$$\begin{aligned}\frac{R_1}{9}&=\frac{1}{3}L_1(0)+\frac{1}{2}L_1(1)+\frac{1}{6}L_1(2)\\&=\frac{1}{3}L_2(0)+\frac{1}{2}L_2(1)+\frac{1}{6}L_2(2),\\\frac{R_2}{9}&=\frac{1}{3}L_1(0)-\frac{1}{2}L_1(1)+\frac{1}{6}L_1(2)=L_2(2),\\\frac{R_3}{9}&=\frac{1}{3}L_2(0)-\frac{1}{2}L_2(1)+\frac{1}{6}L_1(2)=L_1(2)\end{aligned} \tag{A18}$$

are expressed in terms of the Wigner 6j symbols $L_{1,2}$ [65]

$$L_1(k)=\begin{Bmatrix}k & 1 & 1\\ j_2 & j_1 & j_1\end{Bmatrix},\quad L_2(k)=\begin{Bmatrix}k & 1 & 1\\ j_1 & j_2 & j_2\end{Bmatrix}. \tag{A19}$$

The ratio of the Fourier component of the inverse population density of the medium to its average value is [66]

$$N_{12}=\int_0^L N(z)\exp[-2\mathrm{i}(K_1-K_2)z]\mathrm{d}z\Big/\int_0^L N(z)\mathrm{d}z. \tag{A20}$$

Expressions for a_{14}, b_{14}, $\tilde{b}_{14}$, and d_{14} are obtained from expressions for a_{13}, b_{13}, $\tilde{b}_{13}$, and d_{13} by the replacement $\beta_3 \to \beta_4$, $\gamma_3 \to \gamma_4$, $x_{13} \to x_{14}$; the upper sign corresponds to the coefficient a_{1k} and the lower sign – to the coefficient d_{1k}. The nonlinear interaction coefficients for wave 2 are obtained from (A1)–(A20) by the subscript replacements $1 \leftrightarrow 2$ and $3 \leftrightarrow 4$, for wave 3 by the replacement $1 \leftrightarrow 3$ and $2 \leftrightarrow 4$, and for wave 4 by the replacement $1 \leftrightarrow 4$ and $2 \leftrightarrow 3$.

References

1. Privalov V.E., Fridrikhov S.A. *Usp. Fiz. Nauk*, **97**, 374 (1969).
2. Fedorov B.F., Sheremet'ev A.G., Umnikov V.N. *Opticheskii kvantovyi giroskop* (Optical Quantum Gyro) (Moscow: Mashinostroenie, 1973).
3. Azarova V.V., Golyaev Yu.D., Dmittriev V.G. *Kvantovaya Elektron.*, **30**, 96 (2000) [*Quantum Electron.*, **30**, 96 (2000)].
4. Vetkin V.A., Khromykh A.M., in *Kvantovaya Elektronika* (Quantum Electronics), **3** (9), 59 (1972).
5. Sokolov V.A., Fradkin E.E. *Kvantovaya Elektron.*, **2**, 807 (1975) [*Sov. J. Quantum Electron.*, **5**, 447 (1975)].
6. Nazarenko M.M., Savel'ev I.I., Skulachenko S.S. *Kvantovaya Elektron.*, **6**, 1698 (1979) [*Sov. J. Quantum Electron.*, **9**, 1000 (1979)].
7. Yasinskii V.M. *Proc. SPIE Int. Soc. Opt. Eng.*, **2792**, 166 (1995).
8. Yasinskii V.M. *Kvantovaya Elektron.*, **23**, 1086 (1996) [*Quantum Electron.*, **26**, 1056 (1996)].
9. Klimontovich Yu.L., Landa P.S., Lariontsev E.G. *Zh. Eksp. Teor. Fiz.*, **52**, 1616 (1967).
10. Klimontovich Yu.L. (Ed.) *Volnovye i fluktuatsionnye protsessy v lazerakh* (Wave and Fluctuation Processes in Lasers) (Moscow: Nauka, 1974).
11. Chyba T.H. *Phys. Rev. A*, **40**, 6327 (1989).
12. Chyba T.H. *Opt. Commun.*, **76**, 395 (1990).
13. Svirina L.P. *Opt. Commun.*, **111**, 380 (1994).
14. Le Floch A., Ropars G., Lenormand J.M., Le Naour R. *Phys. Rev. Lett.*, **52**, 918 (1984).
15. Cotteverte J.C., Bretenaker F., Le Floch A. *Opt. Lett.*, **16**, 572 (1991).
16. Puccioni J.P., Lippi J.L., Abraham N.B., Arecchi F.T. *Opt. Commun.*, **72**, 361 (1989).
17. Svirina L.P., Gudelev V.G., Zhurik Yu.P. *Phys. Rev. A*, **56**, 5053 (1997).
18. Svirina L.P. *Quantum & Semiclassical Optics, JEOS, part B*, **10**, 425 (1998).
19. Brunel M., Emile O., Alourni M., Le Floch A., Bretenaker F. *Phys. Rev. A*, **59**, 831 (1999).
20. Kravtsov N.V., Lariontsev E.G., Naumkin N.I. *Kvantovaya Elektron.*, **34**, 839 (2004) [*Quantum Electron.*, **34**, 839 (2004)].
21. Klimontovich Yu.L., Kuryatov V.N., Landa P.S. *Zh. Eksp. Teor. Fiz.*, **51**, 3 (1966).
22. Aronowitz F., Collind R.J. *Appl. Phys. Lett.*, **9**, 55 (1966).
23. Fradkin E.E. *Opt. Spektrosk.*, **33**, 674 (1972).
24. Bershtein I.L., Stepanov D.P. *Izv. Vyssh. Uchebn. Zaved., Ser. Radiofiz.*, **16**, 531 (1973).
25. Andronova I.A. *Izv. Vyssh. Uchebn. Zaved., Ser. Radiofiz.*, **17**, 775 (1974).
26. Kutsak A.A., Strekalovskaya E.Yu. *Zh. Prikl. Spektrosk.*, **23**, 995 (1975).
27. Birman A.Ya., Savushkin A.F., Salamatin V.A. *Opt. Spectrosk.*, **53**, 174 (1982).
28. Andronova I.A., Bershtein I.L. *Izv. Vyssh. Uchebn. Zaved., Ser. Radiofiz.*, **14**, 698 (1971).
29. Sardyko V.I., Severikov V.N. *Zh. Prikl. Spektrosk.*, **26**, 826 (1977).
30. Paddon P., Sjerve E., May A.D., et al. *J. Opt. Soc Am. B*, **9**, 574 (1992).
31. Jones R. C. *J. Opt. Soc. Am.*, **31**, 488 (1941).
32. Jones R. C. *J. Opt. Soc. Am.*, **38**, 671 (1948).
33. Jones R. C. *J. Opt. Soc. Am.*, **46**, 126 (1956).
34. Rubanov V.S., Svirina L.P., Severikov V.N. *Dokl. Akad. Nauk BSSR*, **26**, 616 (1982).
35. Il'yushchenko N.V., Svirina L.P., Severikov V.N. *Opt. Spektrosk.*, **54**, 380 (1983).
36. Il'yushchenko N.V., Svirina L.P., Severikov V.N. *Opt. Spektrosk.*, **54**, 874 (1983).
37. Kuznetsov V.M., Rubanov V.S., Svirina L.P., Severikov V.N. *Kvantovaya Elektron.*, **13**, 66 (1986) [*Sov. J. Quantum Electron.*, **16**, 38 (1986)].
38. Voitovich A.P., Severikov V.N. *Lasery s anizotropnymi rezonatorami* (Ansisotropic-Cavity Lasers) (Minsk: Nauka i Tekhnika, 1988).
39. Azzam R.M., Bashara N.M. *Ellipsometry and Polarized Light* (Amsterdam: North-Holland, 1977; Moscow: Mir, 1981).
40. Raterink H.J., Van der Stadt H., Velsel C.H.P., Dijkstra G. *Appl. Opt.*, **6**, 813 (1967).
41. Svirina L.P. *Quantum & Semiclassical Optics, JEOS, part B*, **10**, 213 (1998).
42. Zborovskii V.A., Tiunov E.A., Fradkin E.E. *Izv. Vyssh. Uchebn. Zaved., Ser. Radiofiz.*, **21**, 816 (1978).
43. Pando C.L., Luno Acosta G.A. *Opt. Commun.*, **114**, 509 (1995).
44. Tiunov E.A., Fradkin E.E. *Opt. Spektrosk.*, **44**, 557 (1978).
45. Anishchenko V.S. *Slozhnye kolebaniya v prostykh sistemakh* (Complex Oscillations in Simple Systems) (Moscow: Nauka, 1990).
46. Anischenko V.S. *Dynamical Chaos – Models Experiments. Appearance, Routes Structure of Chaos in Simple Dynamical Systems* (Singapore, World Scientific, 1995).
47. Anishchenko V.S., Vadivasova T.E., Astakhov V.V. *Nelineinaya dinamika khaoticheskikh i stokhasticheskikh sistem* (Nonlinear Dynamics of Chaotic and Stochastic Systems) (Saratov: Saratov State Unversity, 1999).
48. Hilborn R.C. *Chaos Nonlinear Dynamics* (New York, Oxford: Oxford University Press, 1994).
49. Chua L.O., Komuro M., Matsumoto T. *IEEE Trans. Circuits Syst.*, **CAS-33**, 1073 (1986).
50. *Chua's Circuit: A Paradigm for Chaos*. Ed. by R.N. Madan (Singapore: World Scientific, 1993).
51. Svirina L.P. *J. Optics B: Quantum & Semiclas. Opt.*, **3**, S133 (2001).
52. Skryabin D.V., Vladimirov A.G., Radin A.M. *Opt. Commun.*, **116**, 109 (1995).
53. Skryabin D.V., Vladimirov A.G., Radin A.M. *Opt. Spektrosk.*, **78**, 989 (1995).
54. Svirina L.P. *Opt. Spektrosk.*, **95**, 339 (2003).
55. Nikolaev E.V. *Matemat. Sbornik*, **196**, 143 (1995).
56. Avetisov V.A., Gol'danskii V.I. *Usp. Fiz. Nauk*, **166**, 873 (1996).
57. Dmitriev A.S., Kislov V.Ya. *Stokasticheskie kolebaniya v radiofizike i elektronike* (Stochastic Oscillations in Radiophysics and Electronics) (Moscow: Nauka, 1989).
58. Gudelev V.G., Svirina L.P., Zhurik Yu.P. *Proc. SPIE Int. Soc. Opt. Eng.*, **2792**, 119 (1995).
59. Hwang S.K., Gao J.B., Liu J.M. *Phys. Rev. E*, **61**, 5162 (2000).
60. Gao J.B., Hwang S.K., Liu J.M. *Phys. Rev. E*, **82**, 1132 (1999).
61. Butkovskii O.Ya., Brash J.S., Kravtsov Yu.A., Surovyatkina E.D. *Zh. Eksp. Teor. Fiz.*, **109**, 2201 (1996).
62. Kravtsov Yu.A., Kadtke J.B. *Predictability in Complex Dynamical Systems* (New York: Springer, 1999).
63. Svirina L.P. *Opt. Spektrosk.*, **97**, 165 (2004).
64. Van Kampen N.G. *Stochastic Processes in Physics and Chemistry* (Amsterdam: North-Holland Publishing Co., 1981; Moscow: Vysshaya Shkola, 1990).
65. Sobelman I.I. *Introduction to the Theory of Atomic Spectra* (Oxford: Pergamon Press, 1972; Moscow: Fizmatgiz, 1963).
66. Lamb W.E. *Phys. Rev. A*, **134**, 1429 (1964).